Correlates between calcaneal morphology and locomotion in extant and extinct carnivorous mammals

Elsa Panciroli[1*2,3], Christine Janis[3, 4] and Max Stockdale[3]

[1] University of Edinburgh, Edinburgh, UK, [2] National Museum of Scotland, Chambers Street, Edinburgh, UK, [3] University of Bristol, Bristol, UK, [4] Brown

University, Providence, RI, USA.

Short Title: **Carnivoran calcanea and locomotion**

Main correspondent:

Elsa Panciroli

c/o National Museum of Scotland

Natural Sciences Dept.

Chambers Street

Edinburgh

EH1 1JF

07790209252
elsa.panciroli@ed.ac.uk

Abstract

Locomotor mode is an important component of an animal's ecology, relating to both habitat and substrate choice (e.g., arboreal versus terrestrial) and in the case of carnivores, to mode of predation (ambush versus pursuit). Morphological correlates of behaviour can be employed in ecometrics: the study of how the ecomorphology of species within ecosystems can be integrated across time to reveal larger scale processes such as climatic change. Here we examine how the morphology of the calcaneum, the "heel bone" in the tarsus, correlates with locomotion in extant carnivores. We use these correlations to determine the locomotor mode, and hence aspects of the probable palaeobiology, of some extinct taxa.

The calcaneum is an excellent bone to employ in studies of locomotion. Other studies have confirmed the correlation of calcaneal morphology with locomotion behaviour and habitat, and its robust nature and distinctive shape means that it is frequently both preserved and identified in the fossil record. Here we employ linear measurements and 2D geometric morphometrics on a sample of calcanea from 87 extant carnivorans and demonstrate a strong correlation between calcaneal morphology and locomotor mode. We tested for phylogenetic signal using NPMANOVA and maximum likelihood modelling. We tested the reliability of locomotor allocation using NPMANOVA and LDA. The results were largely free from phylogenetic influence, except in the case of the ursids (bears), which clustered together - apart from the other carnivorans - despite occupying a diversity of locomotor modes. Forty-seven extinct carnivorous mammals (including both Carnivora and Creodonta) were then compared with the extant ones, with some interesting determinations. Our results support an arboreal locomotor grade for the early carnivoramorph *Dormaalocyon latouri*, and show that the nimravids (the extinct "false sabertooths"), usually considered to be arboreal, likely occupied a diversity of locomotor modes, including more cursorial (running adapted).

Keywords: Carnivora, ecomorphology, calcaneum, morphometrics, locomotion

Research Highlights

Calcaneal morphology strongly correlates with locomotor grade in Carnivora, largely uninfluenced by phylogenetic signal (except for ursids). *Nimravus brachyops*' distinct calcaneal morphology indicates a more cursorial locomotion than other nimravids.

Introduction

Placental mammalian carnivores today mostly comprise species in the globally distributed order Carnivora. These mammals are characterised by a dental morphology suited to processing flesh, possessing a pair of carnassial teeth comprised from the fourth upper premolars and first lower molars (Nowak, 2005; Goswami, 2010). Carnivorans exhibit a wide array of ecologies, including taxa of carnivorous, omnivorous, and herbivorous diets, and tree-dwellers, runners, and ambulators in their mode of locomotion, as well as diggers and aquatic species (Goswami, 2010). Their evolutionary history stretches back to the generalized paraphyletic assemblage of "Miacoidea" of the late Palaeocene-early Eocene of the Northern Hemisphere (Wesley-Hunt and Flynn, 2005; Eizirik et al., 2010; Smith and Smith, 2010). Many modern carnivoran families appear in the late Eocene, 37-34 mya, and the carnivoran fossil record comprises three times as many extinct species as extant ones (Goswami, 2010), making this a rich order for palaeontological research.

Until the late Eocene the dominant large carnivorous mammals were the Creodonta, traditionally comprising two families: Hyaenodontidae (generally more dog-like forms) and Oxyaenidae (generally more cat-like forms). However, doubts have been cast on the monophyly of this grouping, and Solé (2013) proposed that they should be considered as two separate orders: Hyaenodontida and Oxyaeonodonta. Creodonts are distinguished from carnivorans by more posteriorly positioned carnassials. They were predominantly scansorial to terrestrial, and appear to have occupied similar ecological niches as today's carnivorans, with later taxa exhibiting increasing specialisation towards hypercarnivory (Friscia and Van Valkenburgh, 2010).

Locomotion is one of the key components to understanding the ecology of a mammal, as an animal's movement strongly correlates with other aspects of its behaviour, such as habitat preference. Specialisations for certain locomotor behaviours lead to changes in musculature, limb proportions and osteology, and this correlation between function and form (ecomorphology or ecometrics) can be quantified (Polly, 2007 and 2010; Polly and Sarwar, 2014). Examination of the morphology of extant taxa for which locomotor behaviour is known, allows the inference of the ecomorphology of extinct species (Figuerido et al., 2016).

Previous work has identified distinct locomotor grades in carnivorans (Van Valkenburgh, 1985; Taylor, 1989): arboreal, spending most of their time moving among trees; scansorial, spending a lot of time on the ground yet also able climbers (many felids are scansorial); and terrestrial, spending most of their time on the ground and rarely climbing. Some derived locomotor grades for Carnivora include: cursorial, specialist runners; semi-fossorial, animals that habitually dig for food and/or shelter; and semi-aquatic, animals that spend time, and locomote, both on land and in water. Early carnivoramorphs are understood to have been arboreal/scansorial (Heinrich and Houde, 2006; Solé et al., 2014).

Carnivorous mammals also vary in their stance along a continuum from plantigrade – the primitive mammalian condition - where the entire foot is contact with the ground, to digitigrade, where the carpus and tarsus are raised off the ground and the animal stands on the digits alone (Polly, 2007). Stance relates to locomotion: plantigrade mammals can propel themselves forwards with greater force, whereas a digitigrade stance facilitates speed by increasing the effective length of the distal limb (Polly, 2007). Arboreal forms are generally plantigrade in stance (Taylor, 1989), while an increasingly digitigrade stance is seen in terrestrial and cursorial forms.

Various features of the appendicular skeleton have been used to understand locomotion in carnivoran mammals, including metatarsal to femur ratios (Garland and Janis, 1993), forelimb shape (Janis and Figuirido, 2014; Meachen-Samuels, 2012; Meachen-Samuels and Van Valkenburgh, 2009; Fabre et al., 2015; Taylor 1974), and forelimb elements such as the distal humerus (Andersson, 2004; Figueirido et al., 2015, 2016) However, forelimb morphology can also be influenced by other ecological behaviours, such as feeding. Hind limb morphology has proven to be well correlated with locomotion and stance - particularly the degree of flexion and inversion-eversion of the foot (Taylor, 1970; Polly, 2008) - and less influenced by secondary ecological factors (Polly, 2007; Schutz and Guralnick, 2007; Samuels et al., 2013; Martín-Serra et al., 2014).

The main foot flexion is at the crurotarsal joint between the tibia and the astragalus. Some movement within the tarsus itself – inversion, eversion and flexion - is the generalised condition for mammals (Szalay, 1984); however the degree of movement and correlated morphology is clearly useful in understanding locomotion, making it an ideal focus for study. Being arboreal requires considerable mobility in the hind limb for locomotion in the trees, such as increased inversion-eversion of the foot (Jenkins and McCLearn, 1984; Polly, 2008). However, terrestrial locomotion requires more stability in the hind limb (Taylor, 1989). The influence of size on ankle mobility appears to be less important than previously suspected (Polly, 2008), although larger body size restricts an animal’s ability to climb and move in trees and has implications for the robustness of skeletal elements due to increased loading (Biewener, 1989).

The calcaneum is located in tarsus (Figure 1) where it articulates with the astragalus and cuboid; the generalised mammalian condition is for the calcaneum to have an articulation with the fibula, but this is not the usual condition in placentals, and is not seen in carnivorans. The calcaneum is an ideal bone for study as it is robust and easily identified, with high preservation potential. Biomechanically it is one of key bones for hind limb movement. The gastrocnemius and soleus muscles attach to the distal end of the calcaneal tuber via the Achilles tendon, and so constitute the main in-lever for plantar-flexion in the hind limb, a motion that produces forward thrust in locomotion when the foot is on the ground. As a result, increased length of the calcaneal tuber increases the lever arm of the gastrocnemius and soleus, and a long tuber is associated with terrestrial locomotion, especially cursorial locomotion. The peroneus brevis and peroneus longus attach on the peroneal tubercle of the calcaneum and control flexion and inversion of the foot, and so the peroneal tubercle is usually broader (mediolaterally) in arboreal taxa.

The articulation of the calcaneum and astragalus forms the lower ankle joint (LAJ), and the range of movement in this joint varies considerably in relation to locomotion. Terrestrial and cursorial taxa have a more tightly locked LAJ, while scansorial and arboreal taxa have a LAJ that allows inversion and rotation of the foot (Jenkins and McClearn, 1984).

While there has been research on correlations between the calcaneum and locomotion in various mammal groups including marsupials (Bassarova et al., 2008), armadillos (Jasinski and Wallace, 2014), and apes (Youlatos, 2003), there are few studies that specifically relate to the carnivoran calcaneum, and studies that exist are either restricted taxonomically (Taylor, 1976; Polly, 2008) or geographically (Polly, 2010). Our research is novel in examining calcaneal morphology across the order Carnivora, with an almost global distribution, and with the inclusion of a wide range of fossil carnivore taxa.

Morphometrics, the quantitative study of shape, provides a rigorous approach to understanding the form and variation of living structures that goes beyond simple anatomical observation (Webster and Sheets, 2010). Linear measurements have traditionally been used to capture osteological shape and relative dimensions (Van Valkenburgh, 1985). While the usefulness of this methodology is undoubted, limitations are also recognised: for example the difficulty in capturing complex shapes and angles, and the tendency for linear measurements to be influenced by size (Zelditch et al., 2004). A newer geometric morphometric technique, based on 2D digital landmarking, captures a constellation of osteological points and makes it possible to quantify shape in an inherently multidimensional analysis (Lawing and Polly, 2009; Webster and Sheets, 2010). Geometric morphometrics removes size variables (although it does not account for the effects of allometry), leaving shape as the only remaining variable for analysis. This landmarking technique is particularly suited to the investigation of the relationship between form and function, such as locomotor grade (Fabre et al., 2015), and exploring the role of phylogeny in shape variation (Monteiro and Abe, 1999).

This study investigates how calcaneal morphology relates to locomotion in extant Carnivora and how it can be used to understand the locomotion and ecology of fossil Carnivora and other carnivorous mammals. We discuss to what extent the placement of extinct taxa within the morphospace generated by the living ones can determine their locomotor grade, within the context of considering the potential influences of phylogeny on calcaneal morphology.

Carnivoran families are largely distinguished by their locomotor mode: all procyonids are arboreal or scansorial, all canids are terrestrial - many are cursorial. We are looking for an overriding signal of function in the morphology of the calcaneum. For example, is an arboreal felid (e.g., the clouded leopard, *Neofelis nebulosa*) more similar to a procyonid, and is a cursorial felid (e.g., the cheetah, *Acinonyx jubatus*) more similar to a canid? If we can establish such a signal we have the basis for determining the locomotor mode of extinct taxa, especially those belonging to families where there are no extant members.

After determining the correlates among extant taxa, we introduced extinct taxa. Miacoids are considered polyphyletic, including a number of stem carnivoraforms previously assigned to the genus *Miacis*, but many have been reassigned into distinct separate genera or as basal members of previously described families such as Amphicyonidae (Solé et al., 2014; Tomiya and Tseng, 2016). Like many other “miaciods”, *Dormaalocyon latouri* from the early Eocene of Belgium is a small, long-bodied arboreal/scansorial carnivore (Solé et al., 2014). Below we discuss the extinct groups of carnivorans considered in this analysis, all known from both North America and the Old World (see Table 1)

Amphicyonidae, commonly known as “bear-dogs”, are an important group of carnivorans with their origins in the middle Eocene, persisting into the Pleistocene (Hunt, 1998b). They evolved into a wide range of sizes, and were obligate carnivores: they were mostly plantigrade in their foot posture but some smaller forms may have been digitigrade. Amphicyonids are usually considered to be caniforms, although recent phylogenetic reappraisal suggests they may be a basal carnivoran outgroup to Caniformia (Tomiya and Tseng, 2016).

In addition to “bear-dogs” there were also “dog-bears”, in the extinct subfamily Hemicyoninae within the Ursidae, known primarily from the Miocene. Hemicyonines were carnivorous, and differed from modern bears in their digitigrade foot posture (Hunt, 1998a), implying a more cursorial form of locomotion.

The systematic position of the Nimravidae, the “false sabre-toothed cats”, is uncertain, with some authors suggesting they are closely related to Felidae (Martín-Serra et al., 2014), others that they are the outgroup to the feliform Carnivorans (Wesley-Hunt and Flynn, 2005), or that they may even fall outside of crown Carnivora (Spaulding & Flynn, 2012). We follow Martín-Serra et al., (2014) and place them as the sister-group to Barbourofelidae and Felidae. As their common name suggests, they were superficially cat-like, but generally had shorter legs, more muscular bodies, and shorter tails than extant felids (Martin, 1998a). They are known from the late Eocene and Oligocene. Nimravids have been considered as terrestrial or arboreal in their habits. The members of the family with the longer sabers (the dirk-toothed forms) have been interpreted as plantigrade in foot posture, while those with shorter sabers (the scimitar-toothed forms) have been interpreted as digitigrade (Martin, 1998a).

Previously placed within Nimravidae, barbourofelids were cat-like carnivorans known from the Neogene, and now considered to comprise their own family, more closely related to true felids than were nimravids (Morlo et al., 2004). The Machairodontinae were an extinct subfamily within Felidae, known primarily from the Plio-Pleistocene but with origins in the Miocene. They include the “true” sabre-toothed cats such as the North American *Smilodon populator* and *S.*

fatalis, and the Old World *Amphimachairodus coloradensis* and *Megantereon cultridens*. These cats were robust, and considered to be muscular ambush predators (Martin 1998b).

Materials and Methods

A photographic dataset of 164 calcanea was collected from 132 species of carnivores, including 87 extant Carnivora, 38 extinct Carnivora, and five Hyaenodontida and two Oxyaenida (Table 1). This includes duplicate representatives of some species, depending on availability of specimens. Duplicate specimens are referred to with a numbered suffix (e.g. *Neofelis nebulosa* 2). Where specimens are only identified to genus level, they are referred to with the suffix “sp.” (e.g. *Dinictis* sp.), and where specimens are identified to sub-species level this is also indicated (e.g. *Acinonyx jubatus venaticus*). Calcanea were photographed with a scale bar in anterior, posterior, medial and lateral views. The extant dataset includes members of all of the terrestrial carnivoran families sampled from a broad geographic distribution. Marine Carnivora (pinnipeds) were excluded. For full details of where photographs were obtained see Supporting Information 1 and Acknowledgements.

A supertree was assembled informally for use in comparative phylogenetic methods (Figure 2). This was based primarily on Martín-Serra et al. (2014) and Agnarsson et al. (2009). For more details on tree construction see Supporting Information 2.

Anterior and lateral view photographs were used for analysis (only anterior views were used for digital landmarking), and anterior images were flipped as necessary so that the sustentacular facet was on the left of the photograph, effectively making all specimens left calcanea. Damaged specimens and photographs of low pixel quality were discarded.

Fourteen linear measurements were chosen to capture the relative dimensions of the calcaneum and the ectal and sustentacular facets that form the articulation with the astragalus (Figure 1). Measurements *a* and *l* capture the length of the calcaneal tuber, forming the lever arm of the pes, and *a* also captures the position of the ectal facet, along with *b*. Measurement *b* also reflects the length of the calcaneal head along with *n*, and the latter also relates to the position of the sustentacular facet. Measurements *d*, *c* and *m* capture the breadth of the calcaneal head. The width of the calcaneal tuber is measured mediolaterally and anteroposteriorly using measurements *f* and *g* respectively. Finally the length and width of the sustentacular and ectal facets are measured by *h*, *i*, *j* and *k*, while the width of the cuboid facet is measured by *e*. All of these relate to the degree of movement and rotation possible in the ankle.

The linear measurements were taken using ImageJ (Abramoff et al., 2004) and measurements for each specimen were taken in the same order. The linear measurements were Z-transformed ((*x*-mean)/stdev) to standardise and remove size so that the results would primarily reflect shape. The transformed data were imported into R (R Core Team, 2013), for the conduction of the principle components analysis (PCA).

For the digital landmarking, 162 anterior photographs representing 123 species were selected. Eleven landmarks were chosen (Figure 1) to reflect the length and breadth of the calcaneum, the shape of the calcaneal head, the placement of the sustentacular and ectal facets, and the shape of the tendo calcaneus (the groove for the attachment of the Achilles tendon). Landmarks were digitised in the same order for every specimen using tpsDIG2 (Rohlf, 2004). The landmark data was superimposed using generalised Procrustes analysis, translating and rescaling the landmarks and rotating them into an optimal least-squares alignment. This removes variables of translation, orientation and scale, leaving only differences in shape for analysis.

Principle components analysis was carried out on the landmark data in R (R Core Team, 2013) using the ape (Paradis et al., 2004), moments (Asquith, 2015), and geomorph (Adams and Otarola-Castillo, 2013) packages (see Supporting Information 8 for R code). Thin-plate splines were generated (using the geomorph package (Adams and Otarola-Castillo, 2013)) for the mean of taxa loading at each end of the PC axes (positively and negatively), and to illustrate shape-change between the overall mean shape and the mean calcaneal shape for each locomotor grade.

To test statistical differences between-locomotor grades, one-way non-parametric multivariate analysis of variance (NPMANOVA) with Euclidean distance measure were carried out using PAST (Hammer et al., 2001) on the PCA scores from the linear measurements and the landmarks (see Supporting Information 3). This analysis was repeated with the data binned by phylogenetic groups to evaluate the effect of phylogeny on morphospace occupation. The between-family NPMANOVAs only included Carnivora (except *Dormaalocyon latouri* and *Nothocyon,* as these extinct taxa have not been assigned to a family).

Analysis of variance (ANOVA) was performed on the extant taxa by locomotor grade to determine if there was a statistically significant relationship between principle component scores and locomotor grade, on data corrected to remove the phylogenetic signal. The results showed that both the linear and the landmark data correlate with locomotor mode (see Supporting Information 4).

To visually assess the relationship between phylogeny and locomotion, phylomorphospaces were plotted using the PCA scores (duplicate specimens of the same taxa were removed) using the ape (Paradis et al., 2004), geomorph (Adams and Otarola-Castillo, 2013), phytools (Revell, 2012) and phangorn (Schliep, 2011) packages in R.

Maximum-likelihood models of trait evolution were used to test for phylogenetic signal. PC axes that correlated significantly with locomotor grade were mapped on to the assembled supertree, and then tested for goodness of fit for Brownian-motion, Pagel’s Lambda and Blomberg’s K models, implemented using ape (Paradis et al., 2004) and geiger (Harmon et al., 2008) packages in R. A chi-square test was performed on the output log-likelihood values of each model to determine whether the Pagel’s Lambda model fit the data significantly better than the Brownian motion model, the latter serving as the null hypothesis.

The extant bear species (Ursidae) were found to cluster separately in the morphospace, and so analyses were run with and without their inclusion, in order to assess the effect of phylogeny on the results. The Miocene taxon *Hemicyon ursinus* (Ursidae: Hemicyoninae) is included in all analyses after the removal of the extant bears, as this ‘dog-bear’ is morphologically distinct from extant Ursidae (likely due to its digitigrade stance) and did not cluster with them. PCAs were also carried on the dataset excluding both Ursidae and creodonts, but as excluding creodonts made almost no difference to the remaining taxon placement, these analyses are not included here.

Linear discriminants analysis was also employed to assign taxa to locomotor grades, using the MASS package (Venebles and Ripley, 2002) in R.

Results

The first two principle components (PCs) of the landmark data explain a higher percentage of variance than the first two PCs of the linear measurement data, both with and without the inclusion of the extant ursids. For the entire dataset, the first two landmark PCs account for 53% of the variance (PC 1 = 29%, PC2 = 24%) whereas the first two linear PCs only account for 40% (PC 1 = 22%, PC2 = 18%) (Table 2). With the exclusion of the ursids, the first two landmark PCs account for 52% (PC 1 = 31%, PC2 = 22%) of the variance, and the first two linear PCs account for 38% (PC 1 = 22%, PC2 = 16%) (Table 3).

In the linear data (Figures 3A and B) scansorial taxa are distributed throughout the morphospace, while terrestrial taxa score slightly more positively on PC1. Arboreal taxa score more negatively and cursorial taxa more positively on PC1 axis, separating them from other taxa with almost no overlap. Arboreal taxa also score more negatively than cursorial taxa on PC2 in the linear data morphospace. The morphospaces generated by both linear and landmark data are generally similar in taxon distribution; but in the linear data extant bears fall into a distinct phylogenetic cluster, scoring more negatively on PC1 and positively on PC2 (Figure 3A and Supporting Information 7).

For the linear dataset including bears, increased tuber length (*a, l*) and length from the base of the sustentacular facet to the bottom of the calcaneal head (*n*) load positively on PC1, while the width of the calcaneal head, spanning the sustentacular facet and LAJ (*m*), loads negatively (Figure 4A). Loading negatively on PC2 are increased length of the calcaneal head (*b*), and increased length of the ectal and sustentacular facets (*h*, *j*). PC2 variables load positively for a longer, wider and deeper calcaneal tuber (*a, f, g, l*), with a wider LAJ (*m*) and projecting sustentacular facet (*d*). Calcanea with high scores on PC2 are overall more robust. With the exclusion of the Ursidae, the measurements that load on PC1 remain almost the same, but with different weighting than in the ursid-inclusive dataset (Figure 4C). The main change is measurement *b*, the length of the calcaneal head, which switches from loading positively to loading negatively. PC2 is very different however, loading positively for increased length of the calcaneal head (*b*), length from the base of the sustentacular facet to the bottom of the calcaneal head (*n*), and slight increase in the size of the ectal and sustentacular facets (*h, i, j, k*). An overall increase in the width of the calcaneal tuber and head loads negatively on the PC2 axis (*c, d, e, f, g m*), especially increased projection of the sustentacular facet (*m*). Increased length of the calcaneal tuber also loads negatively on the PC2 axis (*a, l*).

For the landmark data (Figures 3C and D) scansorial taxa are distributed throughout the morphospace, while terrestrial taxa score slightly more negatively on the PC1 axis. Arboreal taxa score negatively on the PC1 axis and cursorial taxa more positively – again with almost no overlap – however for the landmark PCA that includes bears these grades are also separated on the PC2 axis, with arboreal taxa scoring negatively and cursorial more positively. The extant bears score more positively on PC1 and PC2 in the landmark data (Figure 3C and Supporting Information 7).

The thin plate splines in Figure 3C and D indicate that in the landmark dataset excluding Ursidae, a longer calcaneal tuber and lower portion of the calcaneal head below the sustentacular facet load positively on PC1, with the cuboid facet narrow and perpendicular to the long axis of the calcaneum. The calcaneal tuber is shorter, the top of the ectal fact closer to the top of the tuber, and the LAJ and cuboid facet are mediolaterally broader on the negative PC1 axis, with the calcaneal head shorter below the sustentacular facet. Taxa with positive scores on PC2 also have a longer calcaneal tuber, while those in taxa scoring negatively on PC2 the ectal facet appears to sit higher on the tuber, leading to the effective shortening of the calcaneal tuber. The sustentacular facet is quite high on the calcaneum, effectively lengthening the calcaneal head.

In all of the morphospaces there is overlap between arboreal, semi-aquatic and semi-fossorial taxa. Semi-aquatic taxa do not have a clearly defined morphospace occupation, with taxa falling entirely within the morphospace of other grades. In the morphospaces containing the entire dataset, the inclusion of Ursidae, specifically *Ursus maritimus* (polar bear), which is semi-aquatic

(Table 1), provides the only semi-aquatic data point outside the convex hulls generated by the PCA scores of arboreal, semi-fossorial and cursorial taxa.

Thin plate splines generated from the extant taxa with known locomotor grades highlight the main anatomical differences between the mean for each grade from the mean for the whole dataset (Figure 4E). The spline for scansorial taxa does not differ greatly from the mean, as would be expected for this generalist grade. The splines for arboreal and semi-fossorial taxa share some features, with a broader calcaneal head and wider sustentacular facet. The sustentacular facet becomes longer by expanding downwards, while the upper part of the facet remains stationary. This effectively shortens the length of the distal part of the calcaneal head. The calcaneal head also exhibits a more “W-shaped” cuboid facet. In the arboreal form the top of the ectal facet also moves upwards, effectively shortening the lever arm of the calcaneal heel and increasing the articulation surface with the rest of the ankle. The terrestrial and cursorial splines also share common traits, having a more “V-shaped” cuboid facet and a dorsoventrally compressed sustentacular facet (Figure 4E). In the cursorial spline the entire calcaneum is lengthened by the lowering of the ectal facet, effectively lengthening the lever arm of the calcaneal tuber.

Figure 5 shows the placement of the fossil taxa within the convex hulls of the locomotor types of the extant taxa. Some fossil taxa fall outside of the morphospace generated by the extant taxa, more so in the landmark data than the linear. Almost all of the outliers score negatively on PC2 in the linear PCA, positively on PC2 in the landmark PCA. These outlying taxa are mostly amphicyonids and robust machairodontine felids. Although these taxa differ from the extant carnivores in being more robust, with the exception of *Amphicyon major* they do not cluster with the bears when the extant ursids are included in the analysis (see Figures 3A and C, Figure 5 and Supporting Information 7).While most members of Nimravidae included in this analysis fall into the more arboreal/scansorial convex hull, *Nimravus brachyops* appears distinctly more terrestrial than its relatives. This is particularly evident from the landmark PCA morphospace (Figure 5B). The creodonts almost all fall inside the morphospace generated by the extant taxa, except the hyaenodontid *Apterodon gaudryi*, which has scores similar to the felid *Amphimachairodus coloradensis*. The hyaenodonts cluster mostly with terrestrial extant taxa such as *Canis lupus dingo*, *Lynx canadensis* and *Panthera leo*, while the two oxyaenids appear more scansorial and semi-fossorial.

The phylomorphospaces are quite “messy”: there is no noticeable separation in morphospace between Feliformia and Caniformia, and no overriding correlation between locomotor grade and phylogeny (Figures 6 and 7). However there are some clusters, the most notable being Ursidae (Figures 6A and 7A), which occupy a distinct morphospace from the other families, particularly in the linear data. The only ursid that does not follow this pattern is the extinct *Hemicyon ursinus*, which differs from extant ursids in its digitigrade posture. The amphicyonids and procyonids tend to cluster in morphospace, but they do overlap with taxa from other families. In the landmark data, one branch of the felids (*Miracinonyx, Acinonyx* and *Puma concolor*) occupies a different morphospace on the PC1 axis than the rest of Felidae, scoring more positively, while another, the extinct machairodontine felids, score positively on the PC2 axis.

NPMANOVA for between locomotor group difference indicate statistically significant differences between locomotor groups based on shape, with the results being almost identical for the both PCAs (see Supporting Information 3). Most grades appear statistically different from one another, with some interesting exceptions. In the linear PCA the semi-fossorial and semi-aquatic grades do not appear statistically different from the scansorial grade. In the landmark PCA, the semi-aquatic grade does not appear statistically different from either scansorial or terrestrial grades. The NPMANOVA between families indicates a higher statistical difference between families in the landmark PCA scores than in the linear measurement PCA scores. In both datasets, Nandiniidae show the least statistical difference, and Mephitidae, Ailuridae, Barbourofelidae and Eupleridae were also less statistically different from the other families. It should be noted that all of these families are represented by three or fewer specimens, so sample size is likely to have an effect on the results. Ursidae was the most statistically different, being different from every group except Nandiniidae.

The ANOVA results show that PC1 has the most statistically significant relationship with locomotor grade for the linear and landmark PC scores, as does PC2 in the landmark dataset excluding Ursidae (see Supporting Information 4). For the PCA using datasets that include Ursidae, the landmark data failed to find a statistically significant relationship between any of the PC axes and locomotor grade, although PC1 and PC2 had the lowest p-values.

When excluding Ursidae, both datasets have more statistically significant p-values for PC1 and PC2. This indicates that inclusion of bears generates a morphospace that reflects something other than locomotor grade, probably phylogeny.

The PCs statistically significant in the ANOVA were included in maximum likelihood model fitting. The results of modelling imply that the relationship between phylogeny and locomotor traits is not random, as both Pagel's lambda and trend models fit better than the Brownian motion model (randomness) with highly significant chi-squared p-values except for PC2 in the landmark data for the entire dataset, and PC1 in the landmark data excluding extant Ursidae (see Supporting Information 5 for full results). Pagel's lambda results imply that most of the variation in PC1 in both PCAs including Ursidae is accounted for by phylogeny (91% in linear PCA, 96% in landmark) and similarly excluding the extant ursids, although less for the linear data (77% for linear PC1, 96% for landmark PC1). Similarly, most of the variation is accounted for by phylogeny in PC2 (93% in the linear and 92% in landmark PC2 when excluding Ursidae, 94% in PC2 in the data including extant ursids), although the PC2 in the linear data including ursids is only 74%. This is a strong signal. The non-phylogenetic variation in PC1 in the linear data including Ursidae and PC1 in the landmark data excluding them may be accounted for by locomotor grade. However, Blomberg's K values are <1, suggesting that taxa are more different than would be predicted by phylogeny alone (Blomberg et al., 2003). These values are <1 for all axes tested, so despite the Pagel's lambda values, the exact relationship between locomotor function and phylogeny is difficult to ascertain.

The LDA was slightly more successful in predicting the locomotor grades of extant taxa for the dataset excluding Ursidae (see Supporting Information 6). This dataset was therefore used for predicting fossil taxa locomotor grades (Table 4).

Discussion

The findings of this study regarding form and function in the carnivore calcaneum expand upon previous research, which concentrated only on the length of the lever arm (Polly, 2007, 2008 and 2010). The principle component analyses (PCAs) indicate a measurable distinction between arboreal and semi-fossorial versus terrestrial and cursorial morphospaces (Figure 3). The loadings for the linear PCA suggest that this reflects breadth versus length in the calcaneum (Figure 4). Increased length in the calcaneal tuber correlates with more terrestrial and cursorial locomotion due to the resultant increased lever-arm for movement of the foot in a parasagittal plane, while a broader calcaneal head correlates with arboreal and semi-fossorial grades due to a greater amount of muscle attachment on the peroneal tubercle and increased movement in the lower ankle joint to allow inversion-eversion and rotation. Results of NPMANOVA suggestion these distinctions in morphology between locomotor grades are significant and not artefacts of random noise. However phylogeny must also be taken into account when considering calcaneal morphology in Carnivora.

Comparing thin-plate splines for PC1 and PC2 axes (Figure 3C and D) with those for mean locomotor modes (Figure 4E), it is apparent that morphologies with negative loadings on PC1 closely match the mean arboreal spline, and morphologies with positive loadings on PC1 are similar to the mean cursorial shape change spline. PC2 is harder to interpret: but the mean spline for taxa scoring negatively on PC2 in the landmark data excluding Ursidae is more similar to the mean spline for the terrestrial grade, with a straighter cuboid facet that slopes, rather than being either V-shaped (as in the cursorial mean) or W-shaped (as in arboreal, semi-fossorial and semi-aquatic means). In both the terrestrial and cursorial mean splines of vector change from the overall mean (Figure 4E) the sustentacular facet narrows dorsoventrally. However, in the cursorial mean this involves a ‘pinching’ inwards of these landmarks towards the centre of the facet, whereas in the terrestrial mean the bottom edge of the facet lifts upwards. This could reflect a difference in the change in orientation of the facet to produce a slightly different hinge-like joint in these locomotor grades. A three-dimensional analysis may make this change clearer.

The extant Felidae score more positively than Canidae on PC1 in the linear and landmark data excluding Ursidae. This is probably a reflection of heel length in relation to the rest of the calcaneum. Polly (2010) found felids have a higher ratio of calcaneal tuber length to head length than canids. While this would seem to suggest felids are more cursorial than canids, it is possible that the increased tuber length is related to leaping on prey from an ambush position in cats, requiring more “push-off” than running. This distinction between running and leaping may correlate with negative scores on PC2 in the landmark morphospace - in general canids and felids also score differently on this axis.

The widening of the sustentacular facet in arboreal forms is linked to the increased movement in the joint to allow inversion, eversion and rotation in the lower limb, and so arboreal and semi-fossorial taxa both have a wider calcaneal head reflecting the attachment of musculature to the peroneal tubercle. No meaningful inferences can be drawn from the semi-aquatic taxa included in this analysis. Almost all of the semi-aquatic taxa fall within the morphospaces for other locomotor grades (with the exception of *Ursus maritimus*, which clusters with the rest of Ursidae), and the mean thin-plate spline is similar to those for arboreal and semi-fossorial grades. This is possibly due to small sample size, but also, despite being proficient in an aquatic environment, it is possible that none of the semi-aquatic carnivoran families in this dataset (predominantly otters) have become sufficiently aquatic that their calcaneal morphology is radically altered, as seen in marine carnivores (Polly, 2008).

Locomotor grades are a somewhat subjective means of classifying locomotion and may fail to identify more specific traits in an animal’s movement. Complexity in movement was recognised by some of the earliest (and commonly cited) work on carnivore locomotion by Taylor (1970, 1976). Taylor (1976) employed primary and secondary locomotion categories that included “climbing arboreal walking”, and “arboreal and terrestrial walking and jumping”, as primary categories, and “climbing walking”, and “running walking jumping”, as secondary categories. However, it is worth noting that including too many locomotor grades may leave too few taxa in each grade to allow for meaningful statistical analysis.

The results of maximum likelihood models imply that calcaneal morphology is linked with phylogeny to a certain extent (Supporting Information 5). The unusual position of the jaguarundi (*Puma yagouaroundi*) in the landmark PCA – being much closer to the terrestrial serval (*Leptailurus serval*) on PC1 despite being an accomplished tree-climber - may be understood by its phylogenetically close relationship with this taxon. Locomotor grade is influenced by phylogeny to some extent: it is possible that common ancestral morphology may influence placement for some taxa. However this could not be proven definitively in these analyses and was not the main focus of our analyses.

The phylomorphospaces show that most families remain conservative in their range of locomotor types. This is probably linked to body size, particularly for arboreal taxa which must remain small enough to move among trees. Pursuit predators are all larger than 20kg (Carbone et al., 1999), limiting their efficiency as climbers. However, canids and felids exhibit greater locomotor grade diversity than other families in the Carnivora and also have a wider range of body sizes. This implies that body size is an important factor to consider in further analysis of phylogeny and locomotor grade.

Overall, the linear discriminants analysis (LDA) was successful in assigning extant taxa to their locomotor grade (see Supplementary Information 6), suggesting we can place high confidence in the results for fossil taxa (Table 4). However, some fossil taxa were assigned grades that seem unlikely from anatomical observation, such as a semi-fossorial grade for *Smilodon fatalis*. Based on the traces of phylogenetic legacy seen in the phylomorphospaces (Figures 6 and 7) some taxa may be assigned incorrectly because their phylogeny constrains calcaneal shape, placing them closer to the mean for their ancestral shape. It is also probable that some fossil taxa moved in a manner unlike extant taxa, explaining why they fall outside the extant grade convex hulls. The relatively lower occupation of cursorial morphospace by fossil taxa, particularly in the landmark data, supports the suggestion by Anyonge (1996) and Janis and Wilhelm (1993) that few early Carnivora were pursuit predators.

The New World cat *Miracinonyx trumani*, known as the “American cheetah”, occupies a similar morphospace as the extant Old World cheetah *Acinonyx jubatus* (Figures 3 and 5 and Supporting Information 7). Both score more positively on PC2 than *Miracinonyx inexpectus* in the linear data. *M. trumani* is thought to have evolved from *M. inexpectus* (Van Valkenburgh et al., 1990). The puma (*Puma concolor*) is also thought to be closely related to *M. inexpectus* (possibly sharing a common ancestor; Van Valkenburgh et al., 1990). This phylogenetic relationship may explain the placement of these taxa in morphospace, where *M. inexpectus*, *M. trumani* and *P. concolor* cluster together, all scoring positively on PC1. Both morphospaces support the assertion that *M. trumani* was more cursorial than its closest relatives, except for the cheetah (although study of the sacral morphology implies that *M. trumani* did not use its tail for balance during changing direction in locomotion, as seen in the extant cheetah; Harris, 2014).

Nimravus brachyops falls in a more terrestrial morphospace than the other nimravids in our dataset on both landmark and linear PC1 axis (Figure 5). This suggests *N. brachyops* was more cursorial than previously suspected, and possibly a pounce-pursuit predator rather than an ambusher. While previous studies have suggested that this younger nimravid (late Oligocene, as opposed to *Dinictis* and *Holophoneus* which were late Eocene-early Oligocene) may be more terrestrial (Meachen-Samuels, 2012; Samuels et al., 2013), our analyses reflect this more strongly, using only a single, often well-preserved, bone. Other analyses rely on more complete postcrania or complete forelimbs.

The felid *Nimravides* sp. also scores positively on the PC1 axis for linear and landmark data. It falls close to taxa such as *Miracinonyx* and *Acinonyx jubatus*, suggesting that it was also a capable runner.

The machairodontine felid *Megantereon cultridens* falls alongside the extant lion and tiger (*Panthera leo, Panthera tigris sumatrae*) in the linear morphospace (Figure 5 and Supporting Information 7), suggesting a similar ecology to these large extant terrestrial cats - a result supported by previous analyses of the postcrania (Christiansen and Adolfsen, 2007). It scores more positively on PC1 in the linear PCA than any other felid except the cursorial *Acinonyx* and *Miracinonyx,* due to the proportionally long calcaneal tuber, the low upper limit of the ectal facet, and the longer length of the calcaneal head to the base of the sustentacular facet, all of which load heavily for this axis. In the landmark PCA, *M. cultridens* is closer to the generalised terrestrial morphospace (Figure 4). The difference in placement between taxa in the different PCAs highlights one of the potential drawbacks of linear measurement versus 2D shape analysis in understanding form and function, as the loadings for linear measurements may not distinguish similarly proportioned but observably different shapes.

Amphimachairodus coloradensis falls towards the terrestrial/cursorial end of morphospace (Figure 5), which agrees with previous studies which found it was longer-limbed than other machairodontids (Anyonge, 1996). Previous research also distinguishes it from *Smilodon fatalis*, which has been interpreted as an ambush predator (Anyonge, 1996). In this analysis however, *S. fatalis* falls very near *A*. *coloradensis* in the PCA of the linear data. The landmark PCA distinctly separates the two however, with both *Smilodon* species scoring more negatively on PC1. Again this may reflect the detection of a whole shape in landmark analysis versus linear measurement.

Barbourofelis morrisi has been described as “ambulatory”, a category including larger, slow walking or trotting taxa such as extant ursids. Anyonge (1996) generated a morphospace by analysis of limb cross-sections: he showed that *B. morrisi* fell close to ursids, and suggested this was due to *B. morrisi*’s large size and limb proportions, and that it may be useful to compare it with smaller similar ambulators such as the wolverine (*Gula gulo*) or badger (*Meles meles*). These extant taxa fall near *B. morissi* in both PCAs in this analysis (Figure 5 and Supporting Information 7), supporting a slow walking “ambulatory” gait.

Despite the ambulatory locomotion of Ursidae, their inclusion in the dataset did not reflect locomotor grade, as they did not fall near other non-ursid ambulators. Indeed, extant ursids clustered phylogenetically, as the phylomorphospaces make clear (Figure 6 and 7). The PCA calcaneal shapes and mean splines for each PC axis in the PCAs (Figures 3A and C) show how their inclusion dominates whichever quadrant of the morphospace they occupy. This distinction in morphospace probably reflects a distinct ursid plantigrade condition, and so does not prove useful for understanding morphology and ecology in the rest of Carnivora.

The PCAs are more useful than the LDA for understanding locomotion in the robust and/or plantigrade fossil taxa, such as *Smilodon* species, *Megantereon cultridens, Aelurodon ferox*, the amphicyonids, *Mesocyon* sp. and *Hoplophoneus*. These taxa are assigned as semi-fossorial in the LDA, but this is more likely to be a reflection of their overall robustness. Digging species usually exhibit a more robust morphology, so it is likely that these fossil taxa place near them because they are also more robust (for reasons other than digging, including larger body size), and some may be ecological generalists.

Locomotor grades among extant Felidae were the least successfully assigned in the LDA (only 51% of taxa correctly assigned, as opposed to 69% of canids). Bearing this in mind, we must consider both phylogeny (see previously) and other factors such as robustness and stance as factors not accounted for in the results of the LDA.

Dormaalocyon latouri would appear more arboreal than scansorial from our analysis (Figure 5, Table 4), which agrees with anatomical observation by Solé et al. (2014), who noted the possibility for a wide range of movement between the calcaneum and astragalus, and the well-developed peroneal tubercle, which they likened to the morphology of the extant arboreal palm civet, *Nandinia binotata*. This is also significant as *D. latouri* is an early carnivoramorph and so its morphology should be close to the ancestral morphology of crown Carnivora.

Most creodonts display morphologies that indicate they were scansorial or terrestrial (Morlo, 1999; Friscia and Van Valkenburgh, 2010). This is supported by these analyses, with the implication that although creodont locomotion can be understood through comparison with that of extant carnivorans, the inclusion of more refined terrestrial category may be necessary. Morlo (1999) includes “ambulatory” as a sub-category of terrestrial locomotion for some creodont taxa.

The empty space in the PCAs (positive PC2 in the linear data (Figure 5A) and negative PC2 in the landmark data (Figure 5B)) may reflect a trend in locomotor grade in Carnivora away from the ancestral condition, particularly for Canidae and Felidae. This trend is supported by results of the likelihood model test (Supporting Information 5). It is also probable that some fossil taxa occupy morphospace that no longer exists in modern taxa, making interpretation problematic.

Morphology linked to locomotor grade provides a meaningful ecometric trait that can be subject to statistical analysis. Care must be taken to include relevant locomotor categories to capture the variation within the dataset; for example “ambulatory” may be a useful additional locomotor grade, but it is important to ensure the dataset is large and diverse enough to make further subcategorization statistically meaningful. Any quantitative method for assigning locomotion will only be as successful as the dataset and groupings permit; it is always possible that further inclusion of taxa, changes to categorisation, or more detailed analysis of other elements of the skeleton, may provide a more accurate categorization.

The coupling of linear measurement with landmark analysis may help address potential shortcoming of each methodology, for example where complex shapes may be difficult to capture with linear measurements. This methodology also addresses instances where relative lengths may result in misleading morphospace placement, such as the extremely cursorial placement for *Megantereon cultridens* in our analyses. However, 2D landmarking also has its limits, and 3D analysis – such as 3D landmarks (Martín-Serra et al., 2014) or eigensurface analysis (Polly and MacLeod, 2008) - may capture better shape data for analysis, such as changes in facet orientation (for example the sustentacular facet in *Acinonyx*).

Phylogeny influences locomotor grade, but there can still be meaningful assessment of locomotion in fossil taxa through principle component analysis so long as legacy of phylogeny is carefully considered. The link between body size and phylogeny – namely the larger body size in some families, such as Felidae and Canidae - should also be considered when examining the diversity of locomotor grades in different carnivore families.

The low number of fossil taxa falling within the PCA convex hulls created by extant taxa implies the range of extant taxa does not capture the full range of morphologies in extinct ones. Plantigrade stance is not clearly captured by this study, which may explain why many plantigrade fossil taxa with robust morphologies were not clearly resolved in terms of their locomotion, being assigned as scansorial and semi-fossorial despite this being unlikely based on anatomical observation. The inclusion of secondarily plantigrade extant Ursidae did not resolve this, as they cluster phylogenetically.

These analyses show that the calcaneum can provide a useful single indicator of locomotion in fossil taxa. The large size of the dataset in this analysis including both extant and fossil taxa, and the exploration of various statistical and empirical methods to classify fossil taxa into locomotor type, contribute meaningfully to our understanding of the calcaneum within the field of functional morphology.

Author contributions

Acknowledgments

Many thanks to the curators of the museums who allowed us access to collect photographs: Jerry Herman at the National Museum of Scotland (Edinburgh), Aidrian Lister at the Natural History Museum (London), Judy Galkin and Eileen Westwig at the America Museum of Natural History (New York), Jason Head and Ross Secord at the University of Nebraska State Museum, Judy Chupasko and Mark Omura at the Museum of Comparative Zoology (Massachusetts), the Bill Clemens and Pat Holroyd at the University of California Museum of Palaeontology, and Chris Norris at the Yale Peabody Museum, (Connecticut). Thanks to John-Paul Hodnett (St. Joseph's University, U.S.) for kindly donating photographs for our dataset, particularly three *Miracinonyx* specimens. Also gratitude to the Bristol Palaeobiology Research Group as a whole for providing support, and specifically Tom Stubbs for statistical advice and assistance with R codes, and to Mike Benton for his unerringly positive advice. Finally, thank you to Mauricio Anton for permission to use some of his art for figures and in accompanying posters and presentations. A Brown University Bushnell Foundation grant help to fund CMJ in the collection of data.

References

Abramoff MD, Megalhaes PJ, and RAM SJ. 2004. Image processing with ImageJ. Biophotonics International 11:36–42.

Adams DC, Oterola-Castillo E. 2013. Geomorph: an R package for the collection and analysis of geometric morphometric shape data. Methods Ecol Evol 4:393-399.

Agnarsson I, Kutner M, May-Collado LJ. 2009. Dogs, cats, and kin: A molecular species-level phylogeny of Carnivora. Mol Phylogenet Evol 54:726–745.

Andersson MJ. 2004. Elbow-joint morphology as a guide to forearm function and foraging behaviour in mammalian carnivores. Zool J Linn Soc Lond 142:91-104.

Anyonge W. 1996. Locomotor behaviour in Plio-Pleistocene sabre-tooth cats: A biomechanical analysis. J Zool 238:395-413.

Asquith WH. 2015. lmomco---L-moments, censored L-moments, trimmed L-moments, L-comoments, and many distributions. R package version 2.1.4, Texas Tech University, Lubbock, Texas.

Bassarova M, Janis CM, Archer M. 2008. The calcaneum – on the heels of marsupial locomotion. J Mamm Evol 16:1-23.

Biewener AA. 1989. Mammalian terrestrial locomotion and size. Mechanical design principles define limits. Bioscience 39:776–783.

Blomberg SP, Garland T, Ivea AR. 2003. Testing for phylogenetic signal in comparative data: behavioural traits are more labile. Evolution 57:717-745.

Carbone C, Mace GM, Roberts SC, Macdonald DW. 1999 Energetic constraints on the diet of terrestrial carnivores. Nature 402: 286-288.

Christiansen P, Adolfsen JS. 2007. Osteology and ecology of *Megantereon cultridens* SE311 (Mammalia; Felidae; Machairodontinae), a sabrecat from the Late Pliocene – Early Pleistocene of Senéze, France. Zool J Linn Soc Lond 151:833–884.

Cohen KM, Finney SC, Gibbard PL, Fan J-X. 2015. The ICS International chronostratigraphic chart. Episodes 36: 199-204.

Eizirik E, Murphy WJ, Koepfli K, Johnson WE, Dragoo JW, Wayne RK, O'Brien SJ. 2010. Pattern and timing of diversification of the mammalian order Carnivora inferred from multiple nuclear gene sequences. Mol Phylogenet Evol 56:49-63.

Fabre A, Corbette R. Goswami A, Peigné S. 2015. Do constraints associated with the locomotor habitat drive evolution of forelimb shape? A case study in musteloid carnivorans. J Anat 226:596-610.

Figueirido B, Martín –Serra A, Janis CM 2016. Ecomorphological determinations in the absence of living analogs: the predatory behavior of the marsupial lion

(*Thylacoleo carnifex*) as revealed by elbow joint morphology. Paleobiology 42:508-531.

Figueirido, B, Martín-Serra A, Tseng ZJ, Janis CM 2015. Habitat changes and changing predatory habits in North American fossil canids. Nat Commun 6:7976.

Friscia AR, Van Valkenburgh B. 2010. Ecomorphology of North American Eocene carnivores: evidence for competition between Carnivorans and Creodonts. In: Goswami A, Friscia A, editors. Carnivoran Evolution: New Views of Phylogeny, Form and Function. Cambridge, UK: Cambridge University Press. p 311-341.

Garland T, Janis CM. 1993. Does metatarsal/femur ratio predict maximal running speed in cursorial mammals? J Zool 229:133-151.

Goswami A. 2010 Introduction to Carnivora. In: Goswami A, Friscia A, editors. Carnivoran Evolution: New Views of Phylogeny, Form and Function. Cambridge, UK: Cambridge University Press. p 1-24.

Hammer Ø, Harper DAT, Ryan PD. 2001. PAST: Paleontological statistics software package for education and data analysis. Palaeontol Electron 4:9 p.

Harmon LJ, Weir JT, Brook CD, Glor RE, Challenger W. 2008. GEIGER: investigating evolutionary radiations. Bioinformatics 24:129-131.

Harris ASM. 2014. Morphological analysis of the sacrum of big cats: did the extinct “American cheetah” use its tail for balance like the modern African cheetah? Unpublished Honor’s Thesis, Brown University.

Heinrich RE, Houde P. 2006. Postcranial anatomy of *Viverravus* (Mammalia, Carnivora) and implications for substrate use in basal Carnivora. J Vertebr Paleontol 26:422-435.

Hunt RM Jr. 1998b. Amphicyonidae. In: Janis CM, Scott KM, Jacobs LL, editors. Evolution of Tertiary Mammals of North America, vol. 1: Terrestrial Carnivores, Ungulates, and Ungulatelike Mammals. Cambridge, UK: Cambridge University Press. p 196–227.

Hunt RM Jr. 1998a. Ursidae. In: Janis CM, Scott KM, Jacobs LL, editors. Evolution of Tertiary Mammals of North America, vol. 1: Terrestrial Carnivores, Ungulates, and Ungulatelike Mammals. Cambridge, UK: Cambridge University Press. p 174–195.

Janis CM, Wilhelm PB. 1993. Were there mammalian pursuit predators in the Tertiary? Dances with wolf avatars. J Mamm Evol 1:103-125.

Janis CM, Figueirido B. 2014. Forelimb anatomy and the discrimination of predatory strategies in mammalian carnivores: the behavior of the thylacine as a case study. J Morphol 275:1321-1338.

Jasinski SE, Wallace SC. 2014. Investigation into the paleobiology of *Dasypus bellus* using geometric morphometrics and variation of the calcaneum. J Mamm Evol 21:285-298

Jenkins FA, McClearn D. 1984. Mechanisms of hind foot reversal in climbing mammals. J Morphol 182:197-219.

Larviére S, Seddon PJ. 2001. *Vulpes rueppelli.* Mammalian Species 678, 1-5.

Lawing AM, Polly PD. 2009. Geometric morphometrics: recent applications to the study of evolution and development. J Zool 280:1-7.

Martin LD. 1998a. Nimravidae. In Janis CM, Scott KM, Jacobs LL, editors. Evolution of Tertiary Mammals of North America, vol. 1: Terrestrial Carnivores, Ungulates, and Ungulatelike Mammals. Cambridge, UK: Cambridge University Press. p 228-235.

Martin LD. 1998b. Felidae. In Janis CM, Scott KM, Jacobs LL, editors. Evolution of Tertiary Mammals of North America, vol. 1: Terrestrial Carnivores, Ungulates, and Ungulatelike Mammals. Cambridge, UK: Cambridge University Press. p 236-242.

Martín-Serra A, Figuerido B, Palmqvist P. 2014. A three-dimensional analysis of the morphological evolution and locomotor behaviour of the carnivoran hind limb. BMC Evol Biol 14:129

Meachen-Samuels J. 2010. Comparative scaling of humeral cross-sections of felids and canids using radiographic images. J Mamm Evol 17:193–209.

Meachen-Samuels JA. 2012. Morphological convergence of the prey-killing arsenal of sabertooth predators. Paleobiology 38:1–14.

Meachen-Samuels JA, Van Valkenburgh B. 2009. Forelimb indicators of prey-size preference in the Felidae. J Morphol 270:729–744.

Monteiro LR, Abe AS. 1999 Functional and historical determinants of shape in the scapula of Xenarthran mammals: evolution of a complex morphological structure. J Morphol 241:251-263.

Nowak RM. 2005. Walker’s Carnivores of the World. Baltimore, MD: John Hopkins University Press. 309 p.

Paradis E, Claude J, Strimmer K. 2004. APE: analyses of phylogenetics and evolution in R language. Bioinformatics 20:289-290.

Polly PD. 2007. Limbs in mammalian evolution. In: Hall BK, editor. Fins into Limbs: Evolution, Development, and Transformation. Chicago, IL: University of Chicago Press. p 245-268.

Polly PD. 2008. Adaptive zones and the pinniped ankle: A three-dimensional quantitative analysis of carnivoran tarsal evolution. In: Sargis EJ, Dagasto M, editors. Mammalian Evolutionary Morphology: A tribute to Frederick S. Szalay. Dordecht, Germany: Springer. p 197-196.

Polly PD. 2010. Tiptoeing through the trophics: measuring digitigrady in Carnivora for palaeoenvironmental inference. In: Goswami A, Friscia A, editors. Carnivoran Evolution: New Views of Phylogeny, Form and Function. Cambridge, UK: Cambridge University Press. p 374-410.

Polly PD, Macleod N. 2008. Locomotion in fossil Carnivora: an application of eigensurface analysis for morphometric comparison of 3D surfaces. Palaeontol Electron 11:10-13.

Polly PD, Sarwar S. 2014. Extinction, extirpation, and exotics: effects on the correlation between traits and environment at the continental level. Ann Zool Fenn 51:209-226.

R Core Team. 2013. R: A language and environment for statistical computing. R Foundation for Statistical Computing, Vienna, Austria. http://www.R-project.org/

Rohlf FJ. 2004. TpsDig, digitize landmarks and outlines, version 2.0. Department of Ecology and Evolution, State University of New York at Stony Brook. http://life.bio.sunysb.edu/ee/rohlf/software.html

Revell LJ. 2012. Phytools: An R package for phylogenetic comparative biology (and other things). Methods Ecol Evol 3:217-223.

Samuels JX, Meachen JA, Sakai SA. 2013. Postcranial morphology and the locomotor habits of living and extinct carnivorans. J Morph 274:121-146.

Schliep KP. 2011. Phangorn: phylogenetic analysis in R. Bioinformatics 27:592-593.

Schutz H, Guralnick RP. 2007. Locomotor mode in extant and extinct mustelid carnivorans. Zool J Linn Soc Lond 150:895–914.

Smith T, Smith R. 2010. A new genus of “Miacid” carnivoran from the earliest Eocene of Europe and North America. Acta Palaeontol Pol 55:761-764.

Solé, F. 2013. New proviverrine genus from the Early Eocene of Europe and the first phylogeny of Late Palaeocene-Middle Eocene hyaenoodontidans (Mammalia). J Syst Paleontol 11:375—398.

Solé F, Smith R, Coillot T, De Bast E, Smith T. 2014. Dental and tarsal anatomy of ‘*Miacis*’ *latouri* and a phylogenetic analysis of the earliest carnivoraforms (Mammalia, Carnivoramorpha). J Vertebr Paleontol 34:1-21.

Spaulding M, Flynn JJ. 2009. Anatomy of the postcranial skeleton of ‘Miacis’ uintensis (Mammalia: Carnivoramorpha). J Vertebr Paleontol 29:1212–1223.

Szalay FS. 1984. Arboreality: is it homologous between metatherian and eutherian mammals? Evol Biol 18:215-258.

Taylor ME. 1970. Locomotion in some East African viverrids. J Mammal 51:42-51.

Taylor ME. 1974. The functional anatomy of the forelimb of some African Viverridae (Carnivora). J Morphol 143:307–335.

Taylor ME. 1976. The functional anatomy of the hind limb of some African Viverridae (Carnivora). J Mammal 148:227-254.

Taylor ME. 1989. Locomotor adaptations by carnivores. In Gittleman JL, editor. Carnivore Behavior, Ecology, and Evolution. Ithaca, NY: Cornell University Press. p 382-409.

Tomiya S, Tseng ZJ. 2016 Whence the beardogs? Reappraisal of the Middle to Late Eocene ‘*Miacis*’ from Texas, USA, and the origin of Amphicyonidae (Mammalia, Carnivora). R Soc Open Sci 2016 3: 160518.

Van Valkenburgh B. 1985. Locomotor diversity within past and present guilds of large predatory mammals. J Vertebr Paleontol 11:406-428.

Van Valkenburgh B. 1987. Skeletal indicators of locomotor behavior in living and extinct carnivores. J Vertebr Paleontol 7:162-182.

Van Valkenburgh B, Grady F, Kurtén B. 1990. The Plio-Pleistocene cheetah-like cat *Miracinonyx inexpectatus* of North America. J Vertebr Paleontol 10:434-454 p.

Venebles WN, Ripley BD. 2002. Modern Applied Statistics with S. 4th Ed. New York, NY: Springer. 526 p.

Webster M, Sheets HD. 2010. A practical introduction to landmark-based geometric morphometrics. In Alroy J, Hunt G, editors. Quantitative Methods in Paleobiology, The Paleontological Society Papers 16:163-188.

Wesley-Hunt GD, Flynn JJ. 2005. Phylogeny of the Carnivora: basal relationships among the carnivoramorphans, and assessment of the position of 'Miacoidea' relative to Carnivora. J Syst Palaeontol 3:1-28.

Youlatos D. 2003. Calcaneal features of the Greek Miocene primate *Mesopithecus pentelicus* (Cercopithecoidea: Colobinae). Geobios 36:229–239.

Zelditch ML, Swiderski DL, Sheets HD, Fink WL. 2004. Geometric Morphometrics for Biologists: A Primer. San Diego, CA: Elsevier Academic Press. 443 p.

Figure 1: Position of the calcaneum, anatomical nomenclature, and measurements and landmarks used in this study. In (A), (B) and (C) the position of the calcaneum is shaded grey. (C) Anterior view of the calcaneum with anatomical nomenclature as used in this study, abbreviations: a = astragalus, cu = cuboid. (E) The linear measurements

used in this analysis: ***a*** = calcaneal tuber length from top of ectal facet to most uppermost point of calcaneal tuberosity; ***b*** = length from top of ectal facet to base of cuboid facet; ***c*** = projection of peroneal tubercle from midline; ***d*** = projection of sustentacular facet from midline; ***e*** = width of cuboid facet; ***f*** = mediolateral width of calcaneal tuber; ***g*** = anteroposterior width of tuber; ***h*** = length of ectal facet; ***i*** = width of ectal facet; ***j*** = length of sustentacular facet; ***k*** = width of sustentacular facet; ***l*** = tuber length from uppermost projection of sustentacular facet; ***m*** = width of calcaneal head at widest point including sustentacular facet; ***n*** = length from cuboid facet to bottom of sustentacular facet. (F) Landmarks used in this analysis: **1**, uppermost medial point of the calcaneal tuber; **2**, uppermost lateral point of the calcaneal tuber; **3**, point of maximum curvature in tendo calcaneus; **4**, uppermost point of the sustentacular facet; **5**, medial-most point of the sustentacular facet; **6**, lowermost point of the sustentacular facet; **7**, lowermost medial point of the calcaneal head; **8**, lowermost lateral point of the calcaneal head; **9**, mid-point between landmarks 7 and 8 on the anterior edge of the cuboid facet; **10**, lowermost lateral point of the ectal facet; **11**, uppermost point of the ectal facet. Felid by Mauricio Anton with permission. Anatomical images by author.

Figure 2: Informal supertree of Carnivora and Creodonta with estimated branch lengths. Includes only the taxa featured in this study (subspecies specified where known). Image and animal silhouettes by author, geological timeline adapted from Cohen et al., 2015.

Figure 3: Principle components analyses. (A) linear measurements, entire dataset; (B) linear measurements excluding extant Ursidae; (C) landmarks, entire dataset; (D) landmarks excluding extant Ursidae. Extant taxa colour and shape coded by locomotor grade (for colour see online edition, for full labelling of extant taxa see the Supporting Information 7). Where included, bears are circled with dashed line. Calcanea pictured for each axis in linear PCAs are from taxa scoring most positively/negatively for each axis: (A) PC1- = *Tremarctos ornatus 2*, PC1+ = *Acinonyx jubatus*, PC2- = *Leopardus wiedii*, PC2+ = *Ursus americanus 2*. (B) PC1- = *Eira barbara*, PC1+ = *Acinonyx jubatus*, PC2- = *Ischyrocyon sp.*, PC2+ = *Puma yagouaroundi*). Splines on landmark PCA axes are mean of five taxa scoring most positively/negatively for each axis. Splines and calcanea outlines are not to scale.

Figure 4: Loadings for measurements in linear PCA, and thin-shape splines for mean locomotor grades in landmark PCA. See Figure 3 for morphospaces. (A) PC1 loadings for PCA including Ursidae. (B) PC2 loadings for PCA including Ursidae. (C) PC1 loadings for PCA excluding Ursidae. (D) PC2 loadings for PCA excluding Ursidae. Measurements loading positively and negatively for each PC illustrated above and below relevant PC. Highest loading measurements have dashed (red) outline. (E) Thin-plate splines showing relative warp for each locomotor grade from mean.

Figure 5: PCAs excluding extant Ursidae, with labelled fossil taxa and convex hulls of extant taxa locomotor grade morphospace

occupation. (A) Linear measurement PCA. (B) Landmark PCA.

Abbreviations for fossil species: Aelf = *Aelurodon ferox*; Amac = *Amphimachairodus coloradensis*; Ampf = *Amphicyon frendens*; Ampg = *Amphicyon galushai*; Ampl = *Amphicyon longiramus*; Ampm = *Amphicyon major*; Aptg = *Apterodon gaudryi*; Barf = *Barbourofelis fricki*; Barm = *Barbourofelis morissi*; Borp = *Borophagus pugnator*; Cyns = *Cynelos sinapius*; Dap = *Daphoenus* sp.; Dest = *Desmocyon thomsoni*; Din = *Dinictis* sp.; Dinf = *Dinictis felina*; Dinsq = *Dinictis squalidens*; Dips = *Dipsalidictis platypus*; Dorl = *Dormaalocyon latouri*; Eucd = *Eucyon davisi*; Epih = *Epicyon haydeni*; Hemu = *Hemicyon ursinus*; Hop = *Hoplophoneus* sp.; Hopp = *Hoplophoneus primaevis*; Hya = *Hyaenodon* sp.; Hyac = *Hyaenodon crucians*; Hyam = *Hyaenodon montanus*; Isch = *Ischyrocyon* sp.; Meg = *Megantereon* sp.; Megc = *Megantereon cultridens*; Mes = *Mesocyon* sp.; Miri = *Miracinonyx inexpectus*; Mirt = *Miracinonyx trumani*; Mlic = *Megalictis* sp.; Nim = *Nimravides* sp.; Nimb = *Nimravus brachyops*; Not = *Nothocyon* sp.; Paco = *Pachyaena ossifraga*; Pare = *Paratomarctus euthos*; ; Pat = *Patriofelis* sp.; Phl = *Phlaocyon leucosteus*; Pse = *Pseudailurus* sp.; Smif = *Smilodon fatalis*; Smip = *Smilodon populator*; Tepr = *Tephrocyon rurestris*; Thiv = *Thinocyon velox*.

Figure 6: Phylomorphospace of linear measurement PCA (A) including extant Ursidae, (B) excluding extant Ursidae.

Figure 7: Phylomorphospace of landmarks (A) including extant Ursidae, (B) excluding extant Ursidae.

Table 1: Dataset used in this analysis. Gender of specimen included where known. Museum abbreviations: MCZ = Museum of Comparative Zoology, USA; NHM = Natural History Museum London, UK; AMNH (FAM is Frick collection within the AMNH) = American Museum of Natural History; NMB = Natural History Museum Basel, Switzerland; UCMP = University of California Museum of Palaeontology, Berkeley USA; UNSM = University of Nebraska State Museum, USA; RNSB = Institut Royal des Sciences Naturelles de Belgique, Belgium; YPM Yale Peabody Museum, USA. Locomotor grades for extant taxa from Samuels *et al.* (2013) except: *[1] Meachen-Samuels (2010); *[2] Nowak (2005); *[3] Christiansen & Adolfssen (2007); *[4] Solé *et al.* (2014); *[5] Van Valkenburgh (1987); *[6] Larivière and Seddon (2001).

Table 2: Distribution of Principle Component axes for PCA carried out on the whole dataset including extant bears, linear measurement and landmark data. *Percentages are rounded up.

Table 3: Distribution of Principle Component axes for PCA carried out on the dataset excluding extant bears, linear measurement and landmark data. *Percentages are rounded up**.**

Table 4: Results of LDA on PCA excluding Ursidae in allocating locomotor group to fossil taxa. A = arboreal, S = scansorial, T = terrestrial, C = cursorial, F = semi-fossorial, W = semi-aquatic.

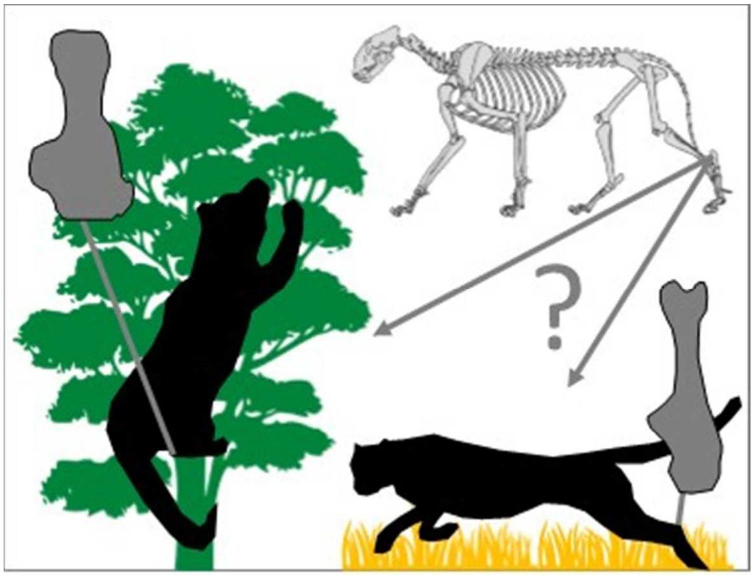

We employ linear measurements and 2D geometric morphometrics to examine how the morphology of the calcaneum, the "heel bone", correlates with locomotion in extant carnivores. We use these correlations to determine the locomotor mode, and hence aspects of the probable palaeobiology, of forty-seven extinct taxa including members of Carnivora and Creodonta.
Graphical Abstract
98x75mm (96 x 96 DPI)

Graphical Abstract

We employ linear measurements and 2D geometric morphometrics to examine how the morphology of the calcaneum, the "heel bone", correlates with locomotion in extant carnivores. We use these correlations to determine the locomotor mode, and hence aspects of the probable palaeobiology, of forty-seven extinct taxa including members of Carnivora and Creodonta.

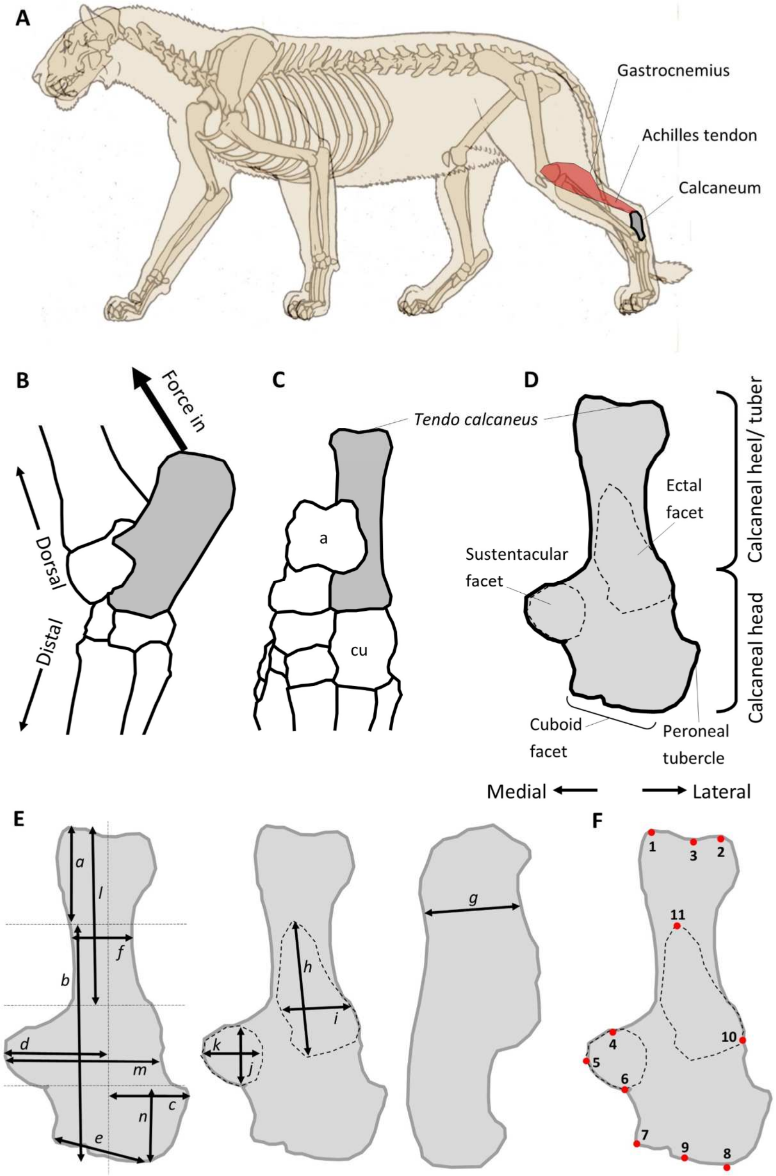

Figure 1: Position of the calcaneum, anatomical nomenclature, and measurements and landmarks used in this study. In (A), (B) and (C) the position of the calcaneum is shaded grey. (C) Anterior view of the calcaneum with anatomical nomenclature as used in this study, abbreviations: a = astragalus, cu = cuboid. (E) The linear measurements used in this analysis: a = calcaneal tuber length from top of ectal facet to most uppermost point of calcaneal tuberosity; b = length from top of ectal facet to base of cuboid facet; c = projection of peroneal tubercle from midline; d = projection of sustentacular facet from midline; e = width of cuboid facet; f = mediolateral width of calcaneal tuber; g = anteroposterior width of tuber; h = length of ectal facet; i = width of ectal facet; j = length of sustentacular facet; k = width of sustentacular facet; l = tuber length from uppermost projection of sustentacular facet; m = width of calcaneal head at widest point including sustentacular facet; n = length from cuboid facet to bottom of sustentacular facet. (F) Landmarks used in this analysis: 1, uppermost medial point of the calcaneal tuber; 2, uppermost lateral point of the calcaneal tuber; 3, point of maximum curvature in tendo calcaneus; 4, uppermost point of the sustentacular facet; 5, medial-most point of the sustentacular facet; 6, lowermost point of the sustentacular facet; 7,

lowermost medial point of the calcaneal head; 8, lowermost lateral point of the calcaneal head; 9, mid-point between landmarks 7 and 8 on the anterior edge of the cuboid facet; 10, lowermost lateral point of the ectal facet; 11, uppermost point of the ectal facet. Felid by Mauricio Anton with permission. Anatomical images by author.

Figure 1

184x274mm (300 x 300 DPI)

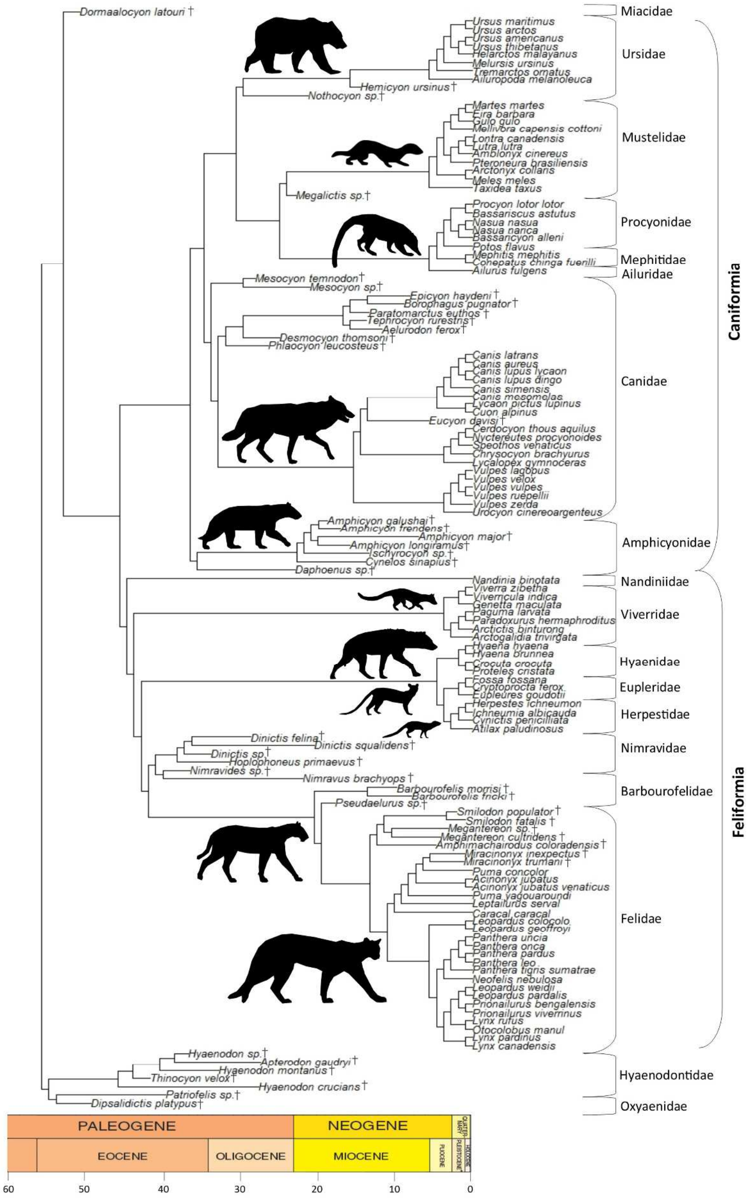

Figure 2: Informal supertree of Carnivora and Creodonta with estimated branch lengths. Includes only the taxa featured in this study (subspecies specified where known). Image and animal silhouettes by author, geological timeline adapted from Cohen et al., 2015.
Figure 2
171x272mm (300 x 300 DPI)

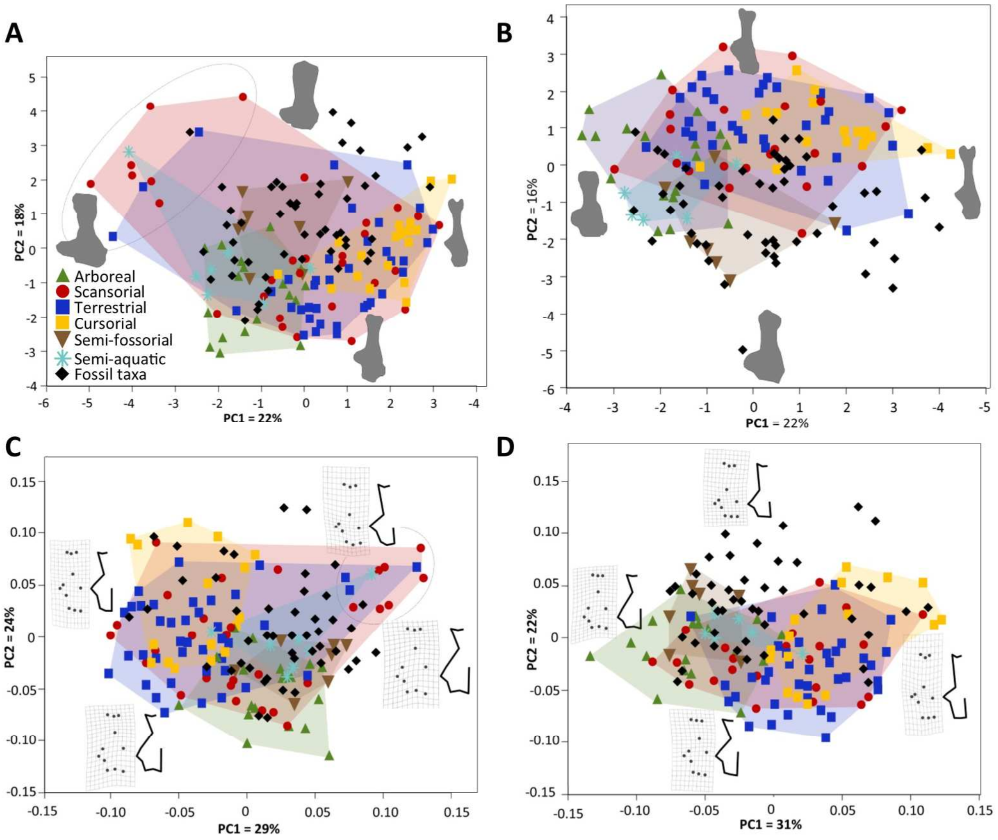

Figure 3: Principle components analyses. (A) linear measurements, entire dataset; (B) linear measurements excluding extant Ursidae; (C) landmarks, entire dataset; (D) landmarks excluding extant Ursidae. Extant taxa colour and shape coded by locomotor grade (for colour see online edition, for full labelling of extant taxa see the Supporting Information 7). Where included, bears are circled with dashed line. Calcanea pictured for each axis in linear PCAs are from taxa scoring most positively/negatively for each axis: (A) PC1- = Tremarctos ornatus 2, PC1+ = Acinonyx jubatus, PC2- = Leopardus wiedii, PC2+ = Ursus americanus 2. (B) PC1- = Eira barbara, PC1+ = Acinonyx jubatus, PC2- = Ischyrocyon sp., PC2+ = Puma yagouaroundi). Splines on landmark PCA axes are mean of five taxa scoring most positively/negatively for each axis. Splines and calcanea outlines are not to scale.

Figure 3

184x154mm (300 x 300 DPI)

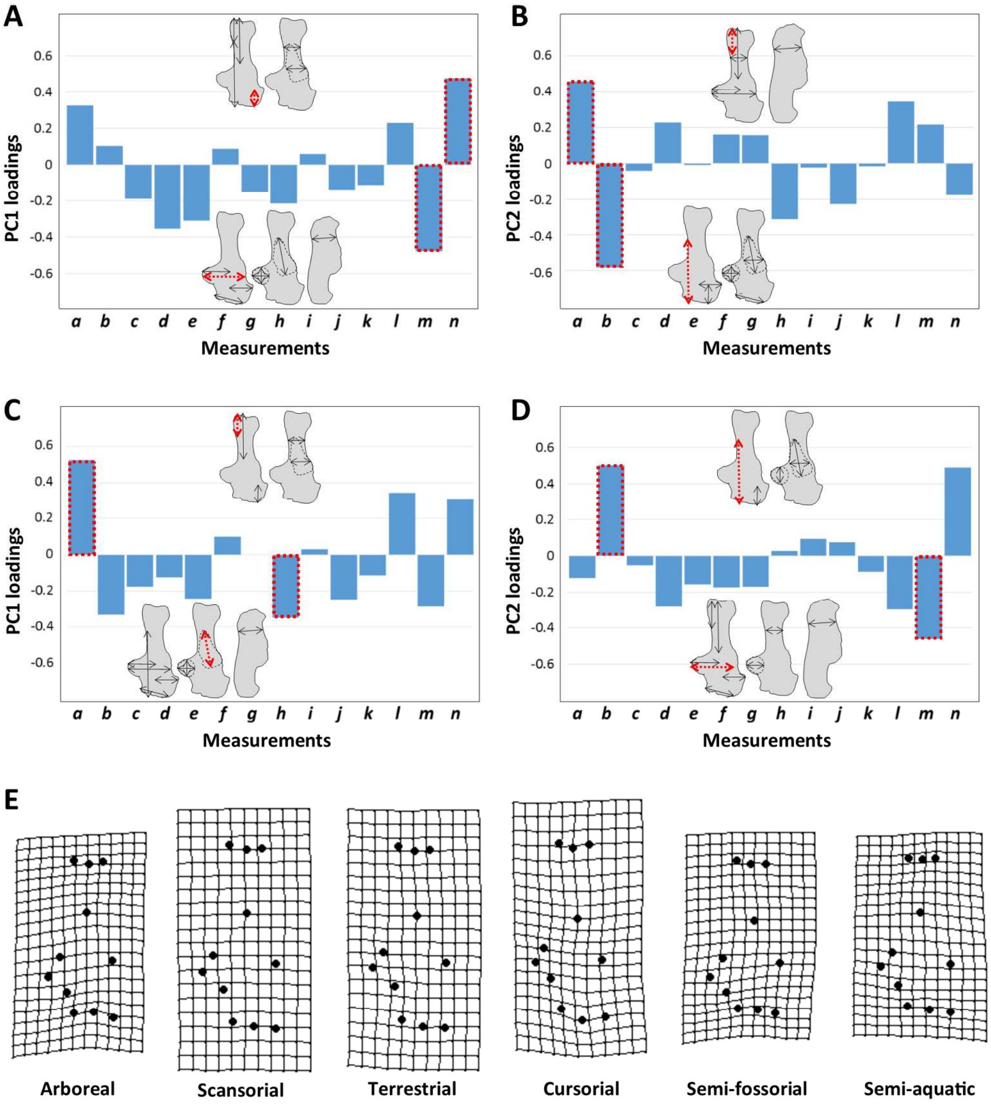

Figure 4: Loadings for measurements in linear PCA, and thin-shape splines for mean locomotor grades in landmark PCA. See Figure 3 for morphospaces. (A) PC1 loadings for PCA including Ursidae. (B) PC2 loadings for PCA including Ursidae. (C) PC1 loadings for PCA excluding Ursidae. (D) PC2 loadings for PCA excluding Ursidae. Measurements loading positively and negatively for each PC illustrated above and below relevant PC. Highest loading measurements have dashed (red) outline. (E) Thin-plate splines showing relative warp for each locomotor grade from mean.

Figure 4

171x193mm (300 x 300 DPI)

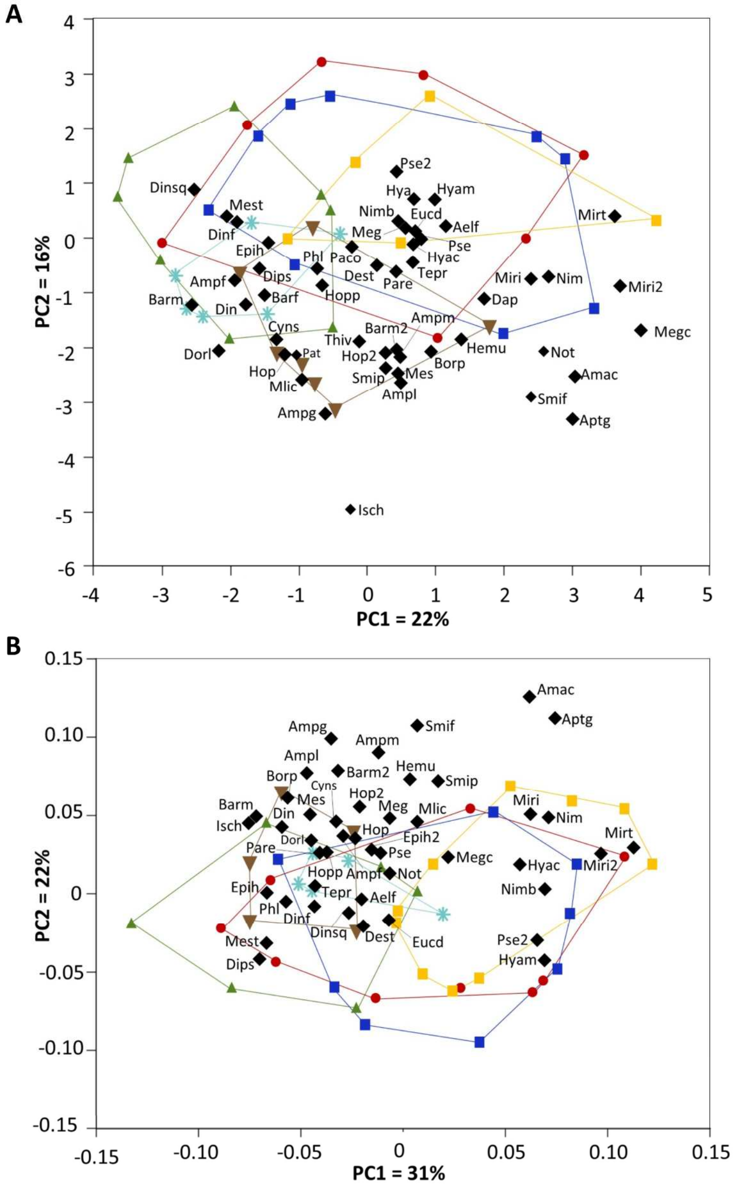

Figure 5: PCAs excluding extant Ursidae, with labelled fossil taxa and convex hulls of extant taxa locomotor grade morphospace occupation. (A) Linear measurement PCA. (B) Landmark PCA. Abbreviations for fossil species: Aelf = Aelurodon ferox; Amac = Amphimachairodus coloradensis; Ampf = Amphicyon frendens; Ampg = Amphicyon galushai; Ampl = Amphicyon longiramus; Ampm = Amphicyon major; Aptg = Apterodon gaudryi; Barf = Barbourofelis fricki; Barm = Barbourofelis morissi; Borp = Borophagus pugnator; Cyns = Cynelos sinapius; Dap = Daphoenus sp.; Dest = Desmocyon thomsoni; Din = Dinictis sp.; Dinf = Dinictis felina; Dinsq = Dinictis squalidens; Dips = Dipsalidictis platypus; Dorl = Dormaalocyon latouri; Eucd = Eucyon davisi; Epih = Epicyon haydeni; Hemu = Hemicyon ursinus; Hop = Hoplophoneus sp.; Hopp = Hoplophoneus primaevis; Hya = Hyaenodon sp.; Hyac = Hyaenodon crucians; Hyam = Hyaenodon montanus; Isch = Ischyrocyon sp.; Meg = Megantereon sp.; Megc = Megantereon cultridens; Mes = Mesocyon sp.; Miri = Miracinonyx inexpectus; Mirt = Miracinonyx trumani; Mlic = Megalictis sp.; Nim = Nimravides sp.; Nimb = Nimravus brachyops; Not = Nothocyon sp.; Paco = Pachyaena ossifraga; Pare = Paratomarctus euthos; ; Pat = Patriofelis sp.; Phl = Phlaocyon leucosteus; Pse = Pseudailurus sp.; Smif =

Smilodon fatalis; Smip = Smilodon populator; Tepr = Tephrocyon rurestris; Thiv = Thinocyon velox.
Figure 5
145x237mm (300 x 300 DPI)

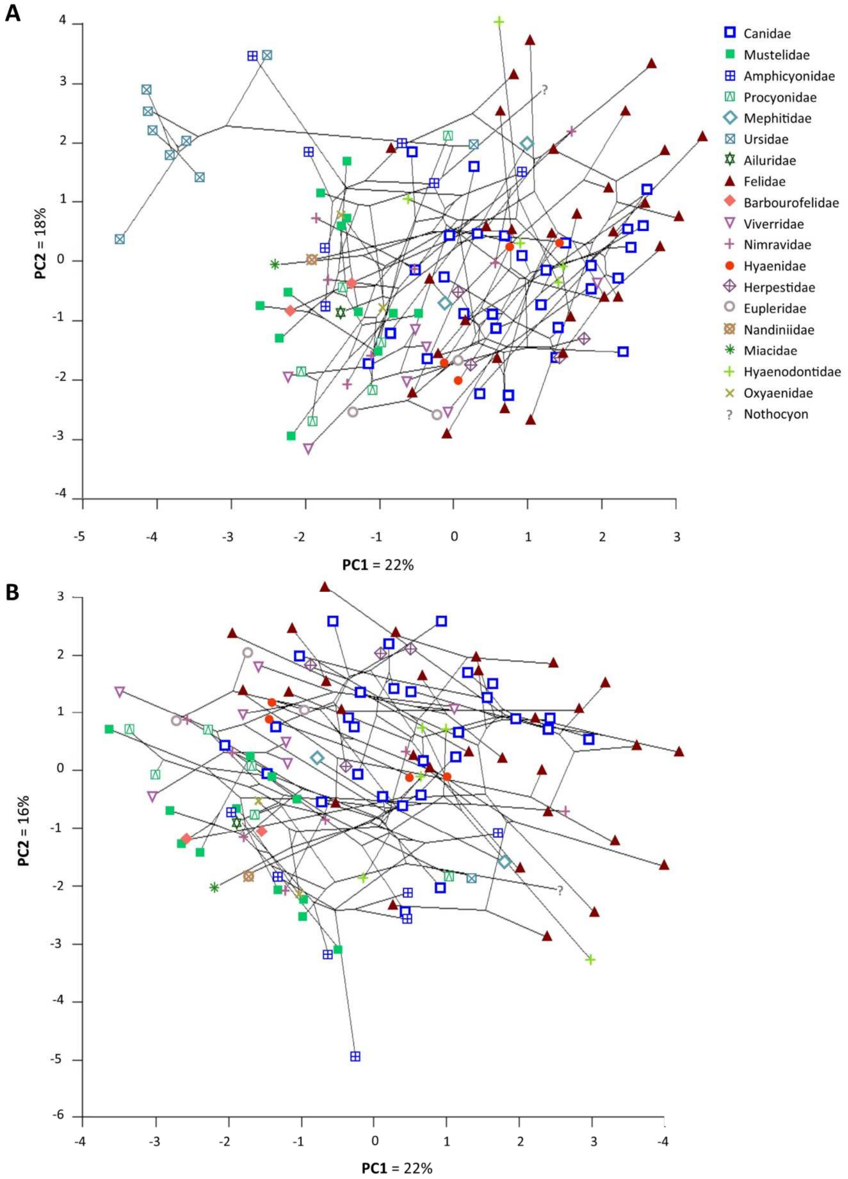

Figure 6: Phylomorphospace of linear measurement PCA (A) including extant Ursidae, (B) excluding extant Ursidae.
Figure 6
182x257mm (300 x 300 DPI)

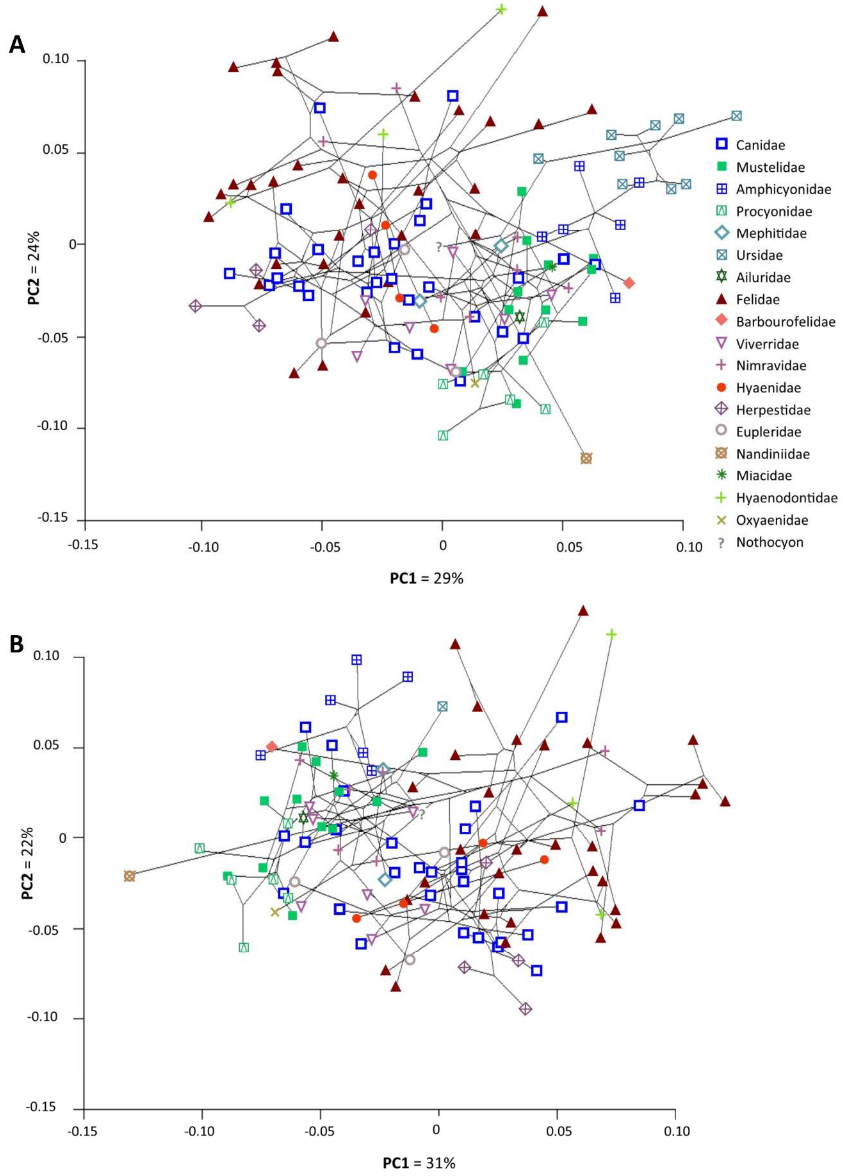

Figure 7: Phylomorphospace of landmarks (A) including extant Ursidae, (B) excluding extant Ursidae.
Figure 7
175x246mm (300 x 300 DPI)

Table 1

	Family	Species	Common name	Extant/ Fossil	Source	Museum Specimen No	♀/ ♂	Locomotor group
Caniformia	**Ailuridae**	*Ailurus fulgens*	Red Panda	Extant	UNSM NMS NMS	17889 Z.1996.139.5 Z.1999.187.3	♀ ♂ ♀	Arboreal
	Amphicyonidae	*Amphicyon frendens*	'Bear-dog'	Fossil	AMNH	68114	-	-
		Amphicyon galushai	'Bear-dog'	Fossil	UNSM	25581	-	-
		Amphicyon longiramus	'Bear-dog'	Fossil	MCZ	4417	-	-
		Amphyicyon major	'Bear-dog'	Fossil	NHM	29620	-	-
		Cynelos sinapius	'Bear-dog'	Fossil	UCMP	JODA 10702	-	-
		Daphoenus sp.	'Bear-dog'	Fossil	AMNH	63343	-	-
		Ischyrocyon sp.	'Bear-dog'	Fossil	AMNH	68156	-	-
	Canidae	*Canis aureus*	Common jackal	Extant	MCZ	9342	-	Terrestrial*[5]
		Canis latrans x2	Coyote	Extant	MCZ MCZ	51124 51692	-	Cursorial
		Canis lupus dingo	Dingo	Extant	MCZ	21590	-	Cursorial
		Canis lupus lycaon x2	Eastern wolf	Extant	MCZ MCZ	56611 56610	♂ ♀	Cursorial
		Canis mesomelas x2	Black-backed jackal	Extant	AMNH MCZ	233010 56858	♂	Cursorial
		Canis simensis	Ethiopian wolf	Extant	AMNH	81001	♂	Terrestrial*[2]
		Cerdocyon thous aquilus	Crab-eating fox	Extant	AMNH	14635	-	Terrestrial
		Chrysocyon brachyurus	Maned wolf	Extant	MCZ	28615	-	Terrestrial
		Cuon alpinus	Dhole	Extant	MCZ	35919	-	Cursorial
		Lycalopex gymnocerus	Pampas fox	Extant	AMNH	205782	♂	Cursorial
		Lycaon pictus lupinus x2	East-African wild dog	Extant	MCZ MCZ	13233 13234	♂ ♂	Cursorial
		Nyctereutes procyonoides	Racoon dog	Extant	MCZ	24860	-	Terrestrial
		Speothos venaticus x2	Bush dog	Extant	MCZ NMS	28056 2015.96.2	- ♀	Terrestrial*[1]
		Urocyon cinereoargenteus x3	Grey fox	Extant	MCZ UNSM UNSM	64708 ZM 14579 ZM 14561	- ♀ ♂	Scansorial
		Vulpes lagopus	Arctic fox	Extant	NMS	JF49.09	♀	Terrestrial
		Vulpes ruepellii	Rüppell's fox	Extant	NMS	DB57.10	♂	Terrestrial*[2]
		Vulpes velox	Swift fox	Extant	UNSM	ZM 14560	♀	Terrestrial*[2]
		Vulpes vulpes	Red fox	Extant	MCZ	64699	♂	Cursorial
		Vulpes zerda	Fennec fox	Extant	NMS	1997.012	♀	Cursorial
		Aelurodon ferox	Borophaginae, 'Bone-crushing dog'	Fossil	AMNH	ZM 17889	-	-
		Borophagus pugnator	Borophaginae, 'Bone-crushing dog'	Fossil	AMNH	FAM 61662	-	-
		Desmocyon thomsoni	Borophaginae, 'Bone-crushing dog'	Fossil	AMNH	49069	-	-
		Epicyon haydeni x2 *(Aelurodon)*	Borophaginae, 'Bone-crushing dog'	Fossil	AMNH AMNH	67703 67704	-	-
		Eucyon (Canis) davisi	Primitive dog	Fossil	AMNH	FAM 63205	-	-
		Mesocyon sp.	Hesperocyoninae	Fossil	MCZ	2885	-	-
		Mesocyon temnodon	Hesperocyoninae	Fossil	AMNH	FAM 63374	-	-
		Paratomarctus euthos	Borophaginae 'Bone-crushing dog'	Fossil	AMNH	61088	-	-
		Phlaocyon leucosteus	Borophaginae 'Bone-crushing dog'	Fossil	AMNH	8768	-	-
		Tephrocyon rurestris	Borophaginae, 'Bone-crushing dog'	Fossil	UCMP	JODA 15283	-	-
	Ursidae	*Ailuropoda*	Giant Panda	Extant	NMS	1986.019	♂	Terrestrial

		melanoleuca						
		Helarctos malayanus	Sun bear	Extant	NMS	Z.2002.066	♂	Scansorial
		Melursus ursinus	Sloth bear	Extant	NMS	R207.00	-	Terrestrial
		Tremarctos ornatus	Spectacled bear	Extant	NMS NMS	2015.19 Z.2004.104	♂ ♀	Scansorial
		Ursus americanus x2	Black bear	Extant	NMS UCMP	- 8817	-	Scansorial
		Ursus arctos	Brown bear	Extant	NMS	Z.2003.41.1		Terrestrial
		Ursus maritimus	Polar bear	Extant	NMS	-	♀	Semi Aquatic
		Ursus thibetanus x2	Asiatic black bear	Extant	NMS UCMP	2002.128.001 131947	♀ -	Scansorial
		Hemicyon ursinus	Hemicyoninae, ‘Dog-bear’	Fossil	AMNH	21101	-	-
	Mephitidae	*Conepatus chinga fuerilli*	Molina’s Hog-nosed skunk	Extant	AMNH	235512	♀	Semi Fossorial*^{2}
		Mephitis mephitis	Striped Skunk	Extant	AMNH	137375	♂	Semi Fossorial
	Mustelidae	*Amblonyx cinereus* x2	Small-clawed otter	Extant	NMS NMS	R123/98 Z.2015.29.2	- ♀	Semi Aquatic
		Arctonyx collaris	Hog-badger (Near threatened)	Extant	AMNH	57118	♂	Semi Fossorial
		Eira barbara	Tayra	Extant	MCZ	30942	-	Arboreal
		Gulo gulo	Wolverine	Extant	AMNH	165766	-	Terrestrial
		Lontra canadensis	Canadian otter	Extant	NMS	GH310.09	-	Semi Aquatic
		Lutra lutra	European otter	Extant	NHM	LY.200 SOC	♂	Semi Aquatic
		Martes martes	Pine martin	Extant	NHM	-	-	Scansorial*^{2}
		Meles meles	European badger	Extant	AMNH	70604	♂	Semi Fossorial
		Mellivora capensis cottoni	Black ratel (honey badger)	Extant	AMNH	51951	♀	Semi Fossorial
		Pteroneura brasiliensis	Giant otter	Extant	NMS	2014.95	♂	Semi Aquatic
		Taxidea taxus x2	American badger	Extant	AMNH UNSM	185259 ZM 27759	♂	Semi Fossorial
		Megalictis sp.	Great weasel	Fossil	AMNH	1598	-	-
	Procyonidae	*Bassaricyon alleni*	Eastern-lowland olingo	Extant	MCZ	37922	-	Arboreal *^{2}
		Bassariscus astutus	Ring-tailed cat	Extant	MCZ	42162	-	Arboreal
		Nasua narica	White-nosed coati	Extant	UNSM	ZM 1135-5	-	Scansorial
		Nasua nasua	South American or ring-tailed coati	Extant	MCZ	1001	♀	Scansorial*^{2}
		Potos flavus	Kinkajou	Extant	MCZ	62043	♂	Arboreal
		Procyon lotor lotor	Eastern Racoon	Extant	MCZ	59137	-	Scansorial
Feliformia	**Barbourofelidae**	*Barbourofelis fricki*	‘False sabre-tooth cat’	Fossil	AMNH	63284	-	-
		Barbourofelis morrisi x2	‘False sabre-tooth cat’	Fossil	AMNH AMNH	FAM 61882 FAM 61883	-	-
	Eupleridae	*Cryptoprocta ferox*	Fossa	Extant	UNSM	ZM 30748	-	Arboreal
		Eupleres goudotii	Falanouc	Extant	MCZ	45960	-	Terrestrial
		Fossa fossana	Fanaloka or Malagasy civet	Extant	MCZ	45966	♀	Scansorial*^{2}
	Felidae	*Acinonyx jubatus* x1 *A. jubatus venaticus*	Cheetah Asiatic cheetah	Extant Extant	MCZ NMS NMS	58142 1996.135 Z.2004.181	- ♀ ♂	Cursorial
		Caracal caracal x2	Caracal	Extant	AMNH MCZ	90105 58305	-	Scansorial*^{1}
		Leopardis colocolo	Andean cat	Extant	AMNH	16695	♂	Scansorial*^{1}
		Leopardis geoffroyi x2	Geoffroy’s cat	Extant	UNSM AMNH	ZM 20845 205991	♂ ♂	Terrestrial*^{1}
		Leopardis pardalis x2	Ocelot	Extant	AMNH UNSM	248728 ZM 15534	♀	Scansorial*^{1}

		Leopardis wiedii	Margay	Extant	UNSM	ZM 14761	♀	Arboreal
		Leptailurus serval	Serval	Extant	AMNH	55041	♂	Terrestrial
		Lynx canadensis x2	Canadian lynx	Extant	MCZ AMNH	7100 22778	 ♀	Terrestrial
		Lynx pardinus	Iberian lynx	Extant	AMNH	169492	♂	Terrestrial*[1]
		Lynx rufus	Bobcat	Extant	MCZ	64140	-	Scansorial
		Neofelis nebulosa x3	Clouded leopard	Extant	AMNH UNSM AMNH	238650 ZM 16951 22919	-	Arboreal
		Otocolobus manul	Pallas's cat	Extant	NMS	2015.65.2	♂	Terrestrial
		Panthera leo	Lion	Extant	MCZ	62919	-	Terrestrial
		Panthera onca	Jaguar	Extant	NHM	117.B	-	Scansorial*[1]
		Panthera pardus	Leopard	Extant	MCZ	13666	-	Scansorial*[1]
		Panthera tigris sumatrae x2	Sumatran tiger	Extant	NMS NMS	Z.2008.023 Z.2013.106	♂ ♀	Terrestrial*[1]
		Panthera uncia x2	Snow leopard	Extant	AMNH NMS	100110 Z.2011.122	♂ ♀	Scansorial
		Prionailurus bengalensis	Leopard cat	Extant	AMNH	238413	♀	Scansorial*[1]
		Prionailurus viverrinus x2	Fishing cat	Extant	NMS NMS	1993.031.003 Z.0996.49.2	♀ ♂	Terrestrial*[2]
		Puma concolor	Cougar	Extant	MCZ	28614	-	Scansorial
		Puma yagouaroundi	Jaguarundi	Extant	MCZ	42787	♀	Scansorial*[1]
		Amphimachairodus coloradensis (Machairodus)	Sabre-tooth cat, Machairodontinae	Fossil	AMNH	FAM 107673	-	-
		Megantereon cultridens	Sabre-toothed cat, Machairodontinae	Fossil	NMB*[3]	SE 311	-	-
		Megantereon sp.	Sabre-toothed cat, Machairodontinae	Fossil	AMNH	105087	-	-
		Miracinonyx inexpectus x2	'American cheetah'	Fossil	UNSM Smithsonian	12866 401092	-	-
		Miracinonyx trumani	'American cheetah'	Fossil	YPM	51665	-	-
		Nimravides sp.	Sabre-toothed cat, Machairodontinae	Fossil	AMNH	21538	-	-
		Pseudaelurus sp. x2	Early cat	Fossil	AMNH AMNH	FAM 62179 2210	-	-
		Smilodon populator (necator)	Sabre-tooth cat, Machairodontinae	Fossil	AMNH	11106	-	-
		Smilodon fatalis (conardi)	Sabre-tooth cat, Machairodontinae	Fossil	AMNH	11792	-	-
	Herpestidae	*Atilax paludinosus*	Marsh/water mongoose	Extant	NMS	R49.01	-	Semi Aquatic
		Cynictis penicilliata	Yellow mongoose	Extant	NMS	PH156.12	-	Terrestrial
		Herpestes ichneumon	Egyptian mongoose	Extant	AMNH	51593	♂	Terrestrial
		Ichneumia albicauda	White-tailed mongoose	Extant	AMNH	35981	-	Terrestrial
	Hyaenidae	*Crocuta crocuta* x2	Spotted hyena	Extant	MCZ Smithsonian	50343 163344	-	Cursorial*[1]
		Hyaena brunnea	Brown hyaena	Extant	UNSM	ZM 16442	-	Terrestrial*[5]
		Hyaena hyaena x2	Striped hyaena	Extant	AMNH Smithsonian	187783 329351	-	Terrestrial*[5]
		Proteles cristata x2	Aardwolf	Extant	AMNH Smithsonian	70261 395686	♀	Terrestrial
	Nandiniidae	*Nandinia binotata*	African or two-spotted palm civet	Extant	AMNH	51469	♀	Arboreal
	Nimravidae	*Dinictis felina*	'False sabre-toothed cat'	Fossil	YPM	10972	-	-
		Dinictis squalidens	'False sabre-toothed cat'	Fossil	AMNH	1386	-	-
		Dinictis sp.	'False sabre-	Fossil	AMNH	38805	-	-

			toothed cat'					
		Hoplophoneus primaevis	'False sabre-toothed cat'	Fossil	AMNH	38980	-	-
		Hoplophoneus sp. x2	'False sabre-toothed cat'	Fossil	UNSM UNSM	25769 48454	-	-
		Nimravus brachyops	'False sabre-toothed cat'	Fossil	AMNH	62151	-	-
	Viverridae	*Arctictis binturong* x2	Binturong	Extant	AMNH UNSM	119600 ZM 15520	-	Arboreal
		Arctogalidia trivirgata	Small-toothed palm civet	Extant	MCZ	35915	♂	Arboreal*[2]
		Genetta maculata	Rusty-spotted genet	Extant	MCZ	38068	♀	Scansorial*[2]
		Paguma larvata	Masked palm civet	Extant	MCZ	36769	♂	Arboreal
		Paradoxurus hermaphroditus	Asian palm civet	Extant	MCZ	38122	-	Arboreal
		Viverra zibetha	Large Indian civet	Extant	MCZ	318121	♂	Terrestrial
		Viverricula indica x2	Small Indian civet	Extant	MCZ MCZ	45984 45985	-	Terrestrial
Other	**Miacoidae**	*Dormaalocyon latouri (Miacis)*	Basal Carnivoramorph	Fossil	RNSB*[4]	M 1360	-	-
	Uncertain (infraorder: Arctoidea)	*Nothocyon* sp.	Early carnivore, related to bears	Fossil	AMNH	49060	-	-
Non-Carnivora	**Hyaenodontida**	*Apteroden gaudryi*	Creodont	Fossil	NHM	M92767	-	-
		Hyaenodont	Creodont	Fossil	UNSM	1-24-7-33SP	-	-
		Hyaenodon crucians	Creodont	Fossil	AMNH	FAM 75729	-	-
		Hyaenodon montanus	Creodont	Fossil	AMNH	FAM75680	-	-
		Thinocyon velox	Creodont	Fossil	AMNH	13082	-	-
	Oxyaenida	*Dipsalidictis platypus*	Creodont	Fossil	AMNH	15857	-	-
		Patriofelis sp.	Creodont	Fossil	YPM	11089	-	-

Table 2

	Linear Measurements			**2D Landmarks**		
	Standard deviation	% Variance*	%* Cumulative	Standard deviation	% Variance*	%* Cumulative
PC1	1.747049	22	22	0.052529	29	29
PC2	1.604368	18	40	0.049097	24	53
PC3	1.197703	10	50	0.031565	10	63
PC4	1.169166	10	60	0.029281	9	72
PC5	1.110084	9	69	0.023436	6	78
PC6	0.999112	7	76	0.020595	4	83
PC7	0.942649	6	82	0.017993	3	86
PC8	0.861535	5	89	0.017456	3	89
PC9	0.848936	5	93	0.014863	2	91
PC10	0.751829	4	97	0.013571	2	93
PC11	0.435967	1	98	0.012386	2	95
PC12	0.424423	1	100	0.011378	1	96
PC13	0.234305	<1	100	0.010299	1	97
PC14	0	0	100	0.00905	1	98
PC15				0.008656	1	99
PC16				0.007319	1	100
PC17				0.005676	<1	100
PC18				0.004501	<1	100
PC19				8.29E-17	0	100
PC20				7.11E-17	0	100
PC21				5.01E-17	0	100
PC22				4.09E-17	0	100

Table 3

	Linear Measurements			**2D Landmarks**		
	Standard deviation	% Variance*	%* Cumulative	Standard deviation	%* Variance	%* Cumulative
PC1	1.743326	22	22	0.051897	31	31
PC2	1.493835	16	38	0.044023	22	52
PC3	1.24155	11	49	0.031662	11	62
PC4	1.192767	10	59	0.025504	7	71
PC5	1.139221	9	68	0.022199	6	77
PC6	1.024582	8	76	0.020785	5	82
PC7	0.952185	7	82	0.017752	4	85
PC8	0.875046	6	88	0.01729	3	89
PC9	0.810484	5	92	0.014937	3	91
PC10	0.752896	4	96	0.012878	2	92
PC11	0.515302	2	98	0.012296	2	95
PC12	0.450632	2	100	0.010982	1	96
PC13	0.229859	<1	100	0.010223	1	97
PC14	0	0	100	0.008782	1	98
PC15				0.00857	1	99
PC16				0.007097	1	99
PC17				0.005765	<1	100
PC18				0.004417	<1	100
PC19				9.03E-17	0	100
PC20				7.44E-17	0	100
PC21				5.26E-17	0	100
PC22				3.27E-17	0	100

Table 4

	Predicted grades	
	Linear	**Landmark**
Amphimachairodus coloradensis	S	C
Megantereon sp.	S	S
Megantereon cultridens	C	C
Miracinonyx inexpectus	C	T
Miracinonyx inexpectus 2	T	T
Miracinonyx trumani	C	C
Pseudailurus sp.	S	C
Pseudailurus sp. 2	T	T
Smilodon fatalis	S	F
Smilodon populator	S	F
Barbourofelis fricki	F	-
Barbourofelis morrisi	F	A
Barbourofelis morrisi 2	S	F
Dinictis felina	T	S
Dinictis squalidens	A	S
Dinictis sp.	S	A
Hoplophoneus primaevis	F	A
Hoplophoneus sp.	T	S
Hoplophoneus sp. 2	S	F
Nimravides sp.	S	C
Nimravus brachyops	T	S
Aelurodon ferox	F	C
Borophagus pugnator	S	F
Desmocyon thomsoni	T	S
Eucyon davisi	T	C
Epicyon haydeni	W	S
Epicyon haydeni 2	W	S
Mesocyon sp.	F	F
Mesocyon temnodon	T	A
Paratomarctus euthos	T	S
Phlaocyon leucosteus	F	C
Tephrocyon rurestris	W	C
Megalictis sp.	T	T
Amphicyon frendens	T	A
Amphicyon galushi	S	F
Amphicyon longiramus	T	F
Amphicyon major	A	F
Cynelos sinapius	A	A
Daphoenus sp.	T	-

Ischyrocyon sp.	S	F
Hemicyon ursinus	S	C
Dormaalocyon latouri	A	A
Apteroden gaudryi	S	F
Hyaenodon crucians	C	T
Hyaenodon montanus	T	T
Hyaenodon sp.	S	-
Thinocyon velox	S	-
Dipsladictis platypus	T	W
Patriofelis sp.	T	-
Nothocyon sp.	T	S